Thermal storage based on phase change materials (PCMs) for refrigerated transport and distribution applications along the cold chain
A review
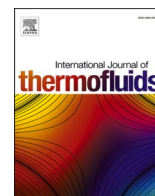
Calati, Michele; Hooman, Kamel; Mancin, Simone

Important note
To cite this publication, please use the final published version (if applicable).
Please check the document version above.

Thermal storage based on phase change materials (PCMs) for refrigerated transport and distribution applications along the cold chain: A review

Michele Calati [a,*], Kamel Hooman [b], Simone Mancin [a]

[a] *University of Padova, Department of Management and Engineering, S.lla San Nicola, 3, Vicenza, 36100, Italy*
[b] *Department of Process and Energy, Delft University of Technology, Delft, the Netherlands*

ARTICLE INFO

ABSTRACT

Foodstuff has to be transported from where it is produced or packaged to the market. It is important to control the temperature and humidity of the delivered food to minimize the waste and ensure customer satisfaction. At the same time, unfortunately, the transport sector is among the polluting sectors. Therefore, innovative solutions have been proposed such as the adoption of Latent Thermal Energy Storage (LTES) systems based on Phase Change Materials (PCMs) to control the food temperature. Such systems minimize the fuel consumption and thereby reduce the emission. LTES systems rely on the phase change process to absorb and store heat in a more sustainable way while ensuring a nearly constant temperature for the foodstuff while being transported.

Hence, we first present a general overview of the application of PCMs at low temperatures. Then, the literature on the adoption of PCMs in the refrigerated transport sector is critically surveyed. Different proposals offered in the literature are recovered, compared, and critically assessed based on their merits. Despite the differences between the proposed technologies, significant advantages in terms of temperature uniformity in the refrigerated space, product thermal stress reduction, product quality, energy consumption, and pollutant emissions reduction are reported in the literature as surveyed in this paper.

Abbreviations

ATP	Accord du Transport Perissable
CFD	Computational Fluid Dynamics
COP	Coefficient of Performance
EC	European Commission
EU	European Union
FAO	Food and Agriculture Organization
FEM	Finite Element Method
GHG	Greenhouse Gas
GWP	Global Warming Potential
HTF	Heat Transfer Fluid
HVAC	Heating, Ventilation and Air Conditioning
ICT	Information and Communication Technologies
IMU	Ice-Making Unit
IN	*Isotherme Normal*
IR	*Isotherme Renforcè*
ISO	International Organization for Standardization
LCA	Life Cycle Assessment
LCCP	Life Cycle Climate Performance
LNG	Liquefied Natural Gas
LTES	Latent Thermal Energy Storage
MCU	Mobile air-Cooling Unit
PCCSU	Phase Change Cold Storage Unit
PCM	Phase Change Material
PCTSU	Phase Change Thermal Storage Unit
PET	Poly-Ethylene Terephthalate
PU	Poly-Urethane
RH	Relative Humidity
RMF	Reflective Multi-Foil
SAP	Super Absorbent Polymer
SDG	Sustainable Development Goal
TES	Thermal Energy Storage
TEWI	Total Equivalent Warming Impact
UN	United Nations
UNI	*Ente nazionale italiano di unificazione*
VIP	Vacuum Insulation Panel

* Corresponding author.
E-mail address: michele.calati@phd.unipd.it (M. Calati).

1. Introduction

It has been estimated that more than 820 million people are malnourished worldwide [1]. In September 2015, the United Nations drew up the seventeen 2030 Sustainable Development Goals (SDGs) [2]. Among the different goals, the second position is the "Zero Hunger" UN program. It can be easily assumed that to reach Goal#2, food losses and food wastages should be prevented. The Food and Agriculture Organization (FAO) [3] evaluated the food wastages and losses in one-third of the total amount of food produced annually, around 1.3 billion ton. In particular, 630 million ton are lost while 670 are wasted [4]. It must be stressed that those numbers are strongly dependent on the countries: for the developed countries a greater contribution is given by the food wastage, while poor or developing countries the food loss component is the prevalent figure. As reported in [4] the food loss is related to a lack of desirable conditions during the first stages of the cold chain, from the producer to the retailer. On the contrary, the food wastage is defined as the edible food being discarded and rejected at the seller and/or customer level.

The cold chain develops from perishable harvested products to the final consumer. It consists of a series of subsequent activities which ensure that fresh foodstuffs are maintained at an adequate temperature throughout the supply chain [2]. The main stages that can be found along the cold chain can be resumed in food harvesting, preconditioning, transport, bulk storage, retail, domestic, and food service [4]. The food losses and wastage add up to $940 billion financial loss per year [5]. Besides, they contribute to the emissions of 4.4 Gton of $CO_{2,eq}$ per year [4]. As stated by Evans et al. [6], if considering both direct and indirect effects, 2.5% of global greenhouse gas (GHG) emissions are due to the cold chain imperfections. The cold chain, in facts, usually adopts refrigeration systems based on high-GWP (Global Warming Potential) refrigerants. It also exploits grid electricity from fossil-fuels or off-grid generation based on diesel equipment [4]. More importantly, the entire refrigeration sector accounts for about 30% of the global energy consumption [7]. Moreover, the world's population is continuously increasing [4] as is the need for welfare. Hence, the European Commission (EC) has been pushing the EU-27 countries in developing solutions aiming at 40% reduction in GHG emissions by 2030 [8]. As reported by Jouhara et al. [9], by adopting energy storage technologies, the goals proposed in the EU's "20–20–20″ program and in the EC's "Energy Roadmap 2050″ can be achieved. In this context, the development and management of a sustainable, effective, and efficient cold chain is becoming more and more crucial. Therefore, with the scope of reducing energy consumption and ensuring an adequate temperature level for the products, among the different Thermal Energy Storage (TES) available, researchers have been considering the introduction of LTES systems to replace the traditional designs along the cold chain. The LTES system takes advantage of the high energy density which can be stored through the phase change process from liquid to solid (or vice versa) at an almost constant temperature [10].

In Fig. 1, demonstrates the great advantage of the use of LTES systems based on PCMs compared with those using a sensible one. The two systems start at the same temperature, but, when the latent system (continuous line) reaches the phase change threshold (T_{pc}) the melting process begins, and the heat storage occurs at an almost constant temperature. Following the completion of the phase change process, liquid PCM stores sensible heat as Fig. 1 depicts. To store the same amount of heat, Q*, the sensible system (dotted line) ends up at a final temperature $T_{sen,end}$ which is noticeably higher than that for a PCM ($T_{lat,end}$). It is clear that a lower system temperature can extend the longevity of the equipment since it can potentially be subjected to lower thermal stresses. This, in turn, lowers the risk of damage and minimizes maintenance costs while improving the system safety and reliability.

The LTESs have already found application in many different contexts as reviewed by Mobedi et al. [10]. These applications range from high temperature industries (electricity generation and waste heat recovery,
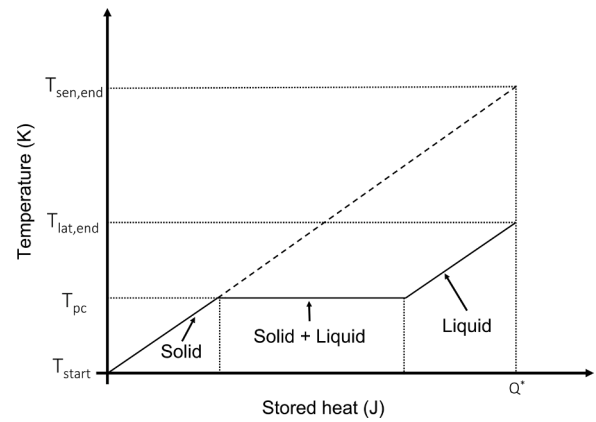

Fig. 1. Comparison between sensible and latent thermal energy storage systems during melting.

[11]), medium temperature applications, from thermal management of electronics and electric vehicle batteries to buildings ([12, 13, 14]and, finally, low and very-low temperature applications such as HVAC systems ([15, 16], Botcher in [10]) or applications for the cold chain [17]. An ideal PCM should have a suitable phase change temperature along with high thermal conductivity and latent heat. It should have low volume expansion and large density in order to limit the system size. The PCM should also be compatible with other materials with no toxicity and flammability [18].

Along the cold chain, the LTESs involving PCMs have already been studied for implementation in commercial and household refrigerating appliances, display cabinets, cold rooms. LTES systems have also started to attract attention for the refrigerated transport sector.

Yusufoglu et al. [19] incorporated different PCMs near the evaporator of two types of refrigerators. They obtained improvement in evaporating and condensing temperatures of 2–4 °C for all the PCM types. Optimizing the on/off compressor times, the LTES prototypes reached energy consumption savings of around 9%. The authors also conducted economic and environmental analyses, stating that the use of PCMs in refrigerators is financially profitable for the users while helping the environment. Ezan et al. [20] placed a PCM (water) slab of different thicknesses (from 2 to 10 mm) on the rear side of a roll-bond evaporator of a vertical beverage cooler. They affirmed that the cooling performance was enhanced in presence of PCM prolonging the compressor "off" duration. Furthermore, during the off interval, the PCM limited the sudden temperature increases thereby maintaining the air inside the refrigerated space at a tolerable range. Pirvaram et al. [21] developed a household refrigerator inserting eutectic PCMs in proximity of a wire-and-tube condenser. The PCM led to a condenser temperature reduction which resulted in the COP enhancement. The cascade arrangement of two PCMs with different melting temperature (29 and 32 °C) permitted the compressor work-on-time to be reduced to 27.6% of total work time (instead of 32.7% for the traditional refrigerator). The authors reported an energy consumption saving of 13%. Gin et al. [22] evaluated the effects of door openings, defrosting cycle and loss of electrical power in a vertical freezer. 2.2 kg of PCM (aqueous ammonium chloride, -15.7 °C) were distributed on the internal cabinet walls, inside aluminum plates. In terms of energy consumption, no differences (without or with PCM cases) were found under steady conditions. However, considering door opening effect, the new solution spared 7–8% of the total energy consumption. When analyzing the occurrence of a loss of power, the great benefit of the developed LTES can be appreciated. The new freezer worked for 11 h until the maximum allowable temperature (-3 °C) was reached whereas the conventional design could only work for 4.4 h before reaching the limit. That is, the new configuration outperformed the traditional one as it maintained operable conditions for a longer period; 2.5 times longer compared with

the traditional vertical freezer. Liu et al. [23] studied the performance of an air-cooled household refrigerator with cold PCMs (0.41 °C melting temperature for cold chamber with -18.98 °C for freezing chamber). They investigated different control modes to report that under the original control mode, the solution with PCM saved 18.6% of energy compared with the reference case. Besides, a 13.6% reduction in the compressor on-time ratio was observed. On top of energy savings, the developed LTES prototype led to better food quality. Orò et al. [24] investigated the thermal performance of a commercial freezer by inserting stainless steel panels encapsulating PCM (-18 °C melting temperature) on the shelves. It was reported that in case of power failure (3 h), the LTES assured a 4–6 °C lower temperature inside the cabinet compared with the traditional design. The PCM prolonged the time the frozen products were maintained at tolerable temperature levels. An 8.6 m^2 cold room based on PCM modules was designed and built by Viking Cold Solutions company [25] for freezing. The TES plates were mounted on top of the stored cargo in the direct path of the airflow generated by the evaporator fans. The LTES system led to an energy consumption reduction of 35% compared to the original setting and the energy consumed during the peak heat load interval reduced by 43%. A warehouse storage for ice cream was numerically studied by Schalbart et al. [26]. They investigated different PCM locations (at the walls, ceiling, close to evaporators, close to products) and reported temperature fluctuations of about ±0.01 °C with PCM in the storage tank against ±1 °C in the situation without PCM over the same period. With the PCM at the ceiling, a difference of ±0.76 °C was reported. The lower temperature differences, the lower the crystal size, with a consequent improvement of the product quality.

In view of the above, given the promising results with the implementation of LTES in refrigerating appliances, researchers have considered introducing them in the refrigerated transport sector. Among the diverse stages along the cold chain, the refrigerated transportation plays an important role as it encompasses initial phases, just after the food harvesting, up to the final ones when it reaches the market. As reported in [27], the retail value of the transported good is about $1200 billion. Nevertheless, it has been forecasted that a growth of 2.5% road cargo transport is expected by 2030 [28]. Thus, as affirmed by De Micheaux et al. [29] the delivery of perishable freight can be considered as the most energy-consuming type of road food transportation. Currently, the refrigerated transportation is regulated by the ATP (*Accord du Transport Perissable*) agreement [30] which defines the standards for refrigerated vehicles. This sector involves 1.2 million refrigerated containers (so called "reefers") and 4 million refrigerated road vehicles [2] of different sizes. The refrigerated road fleet is for the most part equipped with diesel engines which run inefficient mechanical vapor compression cycles for refrigeration [27] their coefficient of performance (COP) usually ranges from 0.5 to 1.5 [31]. According to Li et al. [32], diesel engines consume 1 to 5 liters per hour and that only a quarter of the fuel consumed results into effective work due to engines' low efficiency. It must be stressed that considering the entire amount of energy consumed during the distribution, 40% of it can be ascribed to the food refrigeration [28].

Hence, it is essential for the refrigerated product transportation to move towards solutions which can contemporarily ensure the quality, freshness, and safety of food while meeting the regulations set for the reduction of polluting emissions. In view of the above, the implementation of LTES in the refrigerated transport sector has gained more and more attention by the scientific community.

In this work the state of the art of LTES systems designed for refrigerated transport is reported. In particular, after a general overview of the different PCMs involved in cold latent thermal storages from sub-zero to higher temperatures and a short brief of the refrigerated transport sector to date, a detailed analysis of PCM integration in refrigerated vehicles and portable boxes is offered. The attention is on refrigerated vehicles and portable boxes to analyze the refrigerated transport from the very early stages of the cold chain to the final ones. The literature, in

fact, lacks a complete detailed review specifically devoted to the PCMs integration in applications from big scale transportation (trucks, vans, containers) to small scale distribution (portable boxes). In particular, attention was paid to the typology of the PCM adopted, LTES location, type of insulation material, presence of cold cargo, and the effect of the external temperature and/or solar radiation on the system. The different proposed solutions are cross-compared, and their merits are discussed. Other refrigerating appliances along the cold chain were not considered in this review since many surveys can be retrieved regarding this topic, as discussed in the subsequent chapter. This review identifies the main future challenges for the refrigerated transport sector and offers possible research paths to fill the existing gaps in the literature and facilitate the deployment of LTES in refrigerated transport systems.

2. Reviews from literature and methodology

Several review papers have already been published on the implementation of PCMs along the cold chain. Orò et al. [33] presents a comprehensive review regarding PCMs for cold thermal storage applications. The focus was on the PCMs characterization, unraveling their potential and assessing their drawbacks with little space left for a detailed discussion about the applications. Veerakumar and Sreekumar [34] reviewed cold PCMs dwelling on materials and available solutions to overcome PCM limitations. The refrigerated transport, though, was not considered. Jouhara et al. [9] reviewed different LTES technologies and applications. Moreover, diverse methods of TES (sensible, latent, and thermochemical) were discussed and compared. Nevertheless, PCM for cold chain was not investigated. Cold thermal energy storage applications were considered by Nie et al. [35]. They reviewed latent heat storages with a focus on the material, simulation, and the design work implemented in the cold storage sector. Only a few applications for cold chain transportation were discussed. The research progress of cold storage technology in cold chain transportation and distribution was assessed by Zhao et al. [36]. Several suggested designs were surveyed with a focus on the analysis of the temperature distribution characteristics inside the refrigerated vehicles or containers. Selvnes et al. [37] made a very comprehensive review on cold thermal energy storage applied to refrigeration systems adopting PCMs. Among the different sections, one referring to PCM in refrigerated vehicles and another one concerning the integration of PCM in packaging and containers can be found while the main focus of the work was not on the refrigerated transportation. Yin et al. [38] reviewed cold energy storage and transport but only the ones considering the adoption of hydrates as PCMs. Hameed et al. [39] reviewed the characteristics of low temperature PCMs and presented some applications. Besides, they treated heat transfer enhancement methods and the developed computational techniques to assess, predict, and optimize cold LTES. More recently, Leungtongkum et al. [40] discussed the state of the art of insulated box and refrigerated equipment involving PCM for food preservation. The authors discussed the effect of some influencing factors (such as box shape, insulation material, PCM, operating conditions, etc.) on the modeling. Besides, some cold chain equipment was listed and reviewed.

As seen, introduction of PCMs along the cold chain has been attracting a lot of attention. Nevertheless, as stated in the introductive section, the literature lacks a detailed review covering the PCMs integration in applications from big scale transportation to small scale distribution. Moreover, to help the development of this technology and to encourage the companies to start investing in it, a specific critical discussion of the state of the research is crucial. This is the fundamental brick for a subsequent deployment into real applications, which is essential for the further spreading throughout the market. Therefore, this work aims at filling this gap in the literature.

To focus more specifically on PCM related to the cold chain and, in particular, to the refrigerated transport field, the present authors adopted the following search algorithm: {[(phase change material) OR (latent cold storage)] AND (cold chain)} + {[(phase change material)

OR (latent cold storage)] AND [(refrigerated vehicle) OR (refrigerated truck) OR (refrigerated transport)]} which resulted in about a hundred works. As depicted in Fig. 2, where the annual distribution of published papers from 2000 to 2022 is shown, this topic has gained greater attention in the latest years. In fact, most of the works have been published over the last six years.

Among the papers resulted from the search, the ones that clearly declared the thermo-physical properties of the PCM have been listed in Table 1. To arrange Table 1, the following assumptions were made:

- When there was negligeable difference between melting and solidification temperatures, an average value was reported.
- When only melting or solidification temperature was reported in the work, only the relative column was filled.
- When there was negligeable difference between melting and freezing latent heat values, a unique representative average value was reported.
- When it was not explicitly declared, the thermal conductivity was supposed to be calculated for the solid phase and listed in the relative column.

3. Materials for LTES

The PCM is the main constituent of a LTES system and, as already briefly stated in Section#1, the great benefit of employing a LTES system derives from the exploitation of the latent heat during the liquid-solid phase change transition (and, reverse) of the PCM. Nevertheless, the Energy Storage family also includes [9]: electrochemical and battery, pumped hydro, magnetic, chemical and hydrogen, flywheel, thermochemical, compressed air, liquefied air, and thermal energy storages. Among the thermal ones, sensible and latent storages systems are set as subcategories. Considering LTES, according to their chemical composition, three macro-PCM-categories can be identified:

- *Organic*: organic compounds, paraffins, and fatty acids,
- *Inorganic*: salt hydrates and metallics,
- *Eutectic*: obtained by creating a new PCM starting from at least two different materials. Depending on the nature of the pure constituents, they can be classified as organic-organics, organic-inorganics, or inorganic-inorganics.

In Fig. 3, the latent heat at a determined phase change temperature for all the PCMs listed in Table 1 is plotted. It can be noticed that most of the cold PCM fall into the organic category. Between -10 °C and 10 °C most of the PCMs can be found, with latent heat values ranging from 150 to 250 kJ kg^{-1}. Very low temperatures (under -20 °C) seem to be exclusive prerogative of inorganic and eutectic compounds.

Nevertheless, selection of suitable PCM candidates for a given application should be performed by trying to take into consideration

specific criteria in accordance with the PCM properties, as illustrated by Fig. 4.

Regardless of the different nature of PCM, the ideal one should exhibit an appropriate phase change temperature and a high latent heat value. It should have a high thermal conductivity to improve the heat transfer during the charging/discharging processes. A high-density value is desired since it implies a reduction of the system size (i. e. the same storable mass with a lower occupied volume). The volume change during the phase change should be prevented. The PCM should present homogenous properties, having low vapor pressure at operating conditions. For what concerns the PCM chemical composition, it should perform reversible solidification and melting cycles, being long-term stable at the same time. Moreover, the PCM should be compatible with its TES material, nontoxic, and nonflammable. During the solidification phase, the subcooling phenomenon should be avoided and a good crystal development rate is required. From an economical and environmental aspect, the PCM should be abundant and available in the market at a reasonable price. If possible, the ideal PCM should be recyclable, in order to make this technology environmentally friendly and sustainable, and easy-to-manage with insignificant decommissioning cost for the system.

As anticipated, a PCM matching all these requirements cannot be found [18] thereby a choice based on a trade-off is inevitable. Therefore, based on what reported in Table 1 and [9,18] the advantages and disadvantages of the PCM classes are listed and demonstrated in Fig. 5.

From what reported in Fig. 5 and Table 1, it can be noticed that the main concerns regarding the adoption of PCM based LTES are related to limited thermal conductivity (most of the values range from 0.1 to 1 W m^{-1} K^{-1}), the subcooling phenomenon during the solidification process, an incongruent melting which can result in phase segregation, possible leakage occurring during the melting process, long-term stability, and corrosion. Moreover, the negative effects on human health and the environmental and economic aspects must be carefully managed. Thus, in subsequent sections, the main drawbacks associated with proposed solutions are reported.

3.1. Low thermal conductivity

As stated by Nie et al. [35], a high thermal conductivity is necessary, in order to limit the required time to complete the phase change process. The PCM thermal conductivity can be enhanced with the insertion of high thermal conductivity additives, as composite ones [73] or capsules [106], or they can be devoted to the extension of the heat transfer area [12].

PCM nanocomposites are a very common strategy to solve the thermal conductivity issue. Liu et al. [73] added 1 wt.% multi wallet carbon nanotubes (MWCNTs) into OP5E which is a paraffin based PCM with a phase change temperature between 5 °C and 6 °C. The authors reported that the thermal conductivity increased from 0.20 to 0.37 W
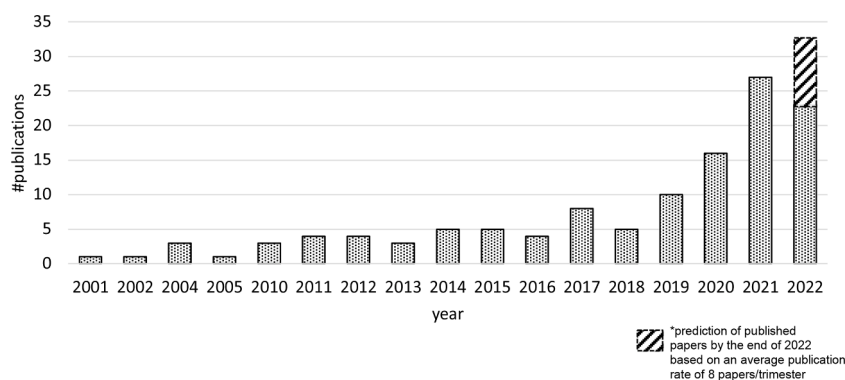

Fig. 2. Number of publications per year (updated to Sep 10th, 2022).

Table 1
PCMs main thermo-physical properties for the cold chain.

Authors	PCM name	Typology	Supplier	Melting Temperature, Tm (°C)	Freezing Temperature, Ts (°C)	Latent heat of phase change, L (J kg⁻¹)	Thermal conductivity, k (W m⁻¹ K⁻¹) solid	liquid
[41]	aqueous-glycol 50%	inorganic		-43.16	-48.16	240,000	2.25	0.35
[42]	organic compound	organic		-6.9		249,000		
[43]	25PCM (microencapsulated PCM, MPCM6D) in a water-based pulp solution (5%w/v)	organic	Microteklabs, USA	4.34	-1.66	55,000	0.0913	0.0913
	50PCM (microencapsulated PCM, MPCM6D) in a water-based pulp solution (5%w/v)	organic	Microteklabs, USA	5.84	-1.66	88,000	0.0819	0.0819
	100PCM (microencapsulated PCM, MPCM6D) in distilled water	organic	Microteklabs, USA	5.84	-2.66	142,700		
[44]	RT-2	organic	Rubitherm, DE	-1.5	-1.5	130,000	0.25	0.2
	RT-4	organic	Rubitherm, DE	-3.1	-3.1	130,000	0.25	0.2
	water-glycol 10%	eutectic		-3	-3	334,000	2.18	0.58
[45]	erythritol tetra myristate ester	organic		10.82	4.76	181,000 (m); 174,450 (f)	0.16	0.16
	erythritol tetra laurate ester	organic		-9.03	-12.86	173,840 (m); 170,760 (f)	0.14	0.14
	erythritol tetra myristate ester+EG (wt5%)	organic		10.67	4.64	161,390 (m); 150,520 (f)	0.18	0.18
	erythritol tetra laurate ester+EG (wt5%)	organic		-8.94	-12.14	156,430 (m); 145,490 (f)	0.2	0.2
[46]	RT5	organic	Rubitherm, DE	6.52	5.26	142,230		
[47]	n-tetradecane	organic	Aladdin, CHN	7.3	4.2	211,000		
[48]	n-hexadecane	organic		15.92	13.37	226,800		
	n-octadecane	organic		25.48	24.59	233,430		
[49]	RT5HC	organic	Rubitherm, DE	6	5	250,000	0.2	0.2
[50]	paraffin	organic		6	2	214,000		
				9	6	174,000		
				9	7	190,000		
				9	8	210,000		
				10	9.9	207,000		
[51]	Microencapsulated PCM (MPCM) in water, slurry	–		28	27	167,000	0.31	0.14
[52]	octadecane	organic	Sigma-Aldrich, USA	28.1		210,000		
[53]	NaCl-Na2SO4 ternary salt in water	eutectic		-21.5		180,000		
	NaCl-KCl ternary salt in water	eutectic		-23		260,000		
	NaCl-NaNO3 ternary salt in water	eutectic		-26.5		100,000		
[54]	octanoic acid lauric acid + expanded graphite 7wt% (OA-LA/EG)	organic		3.6		132,800	1.275	
[55]	dodecane	organic		-8.09		175,900	0.14	0.14
	dodecane/EG 16wt%			-8.46		151,700	2.2745	2.2745
[56]	octaonic acid myristic acid (MA)	eutectic		7.13		146,100	0.2971	0.2971
	octaonic acid myristic acid + expanded graphite 7wt% (OA-MA/EG)	eutectic		6.8		136,300	0.9975	0.9975
[57]	OM11, fatty acid based ester	organic	M/s Pluss Advance Tecnhologies, Ltd., India	9.4		147,490		
[58]	23wt% MgCl2-H20 eutectic salt solution + 1wt% MWCNTs	eutectic		-34.54		146,960	0.5344	
[59]	eutectic salt	eutectic		-5.02		208,300	0.67	
	eutectic salt + modified expanded graphite (MEG)	eutectic		-5.3		161,800	8.9	
[60]	decanoic-caprylic acid (DA-CA)	eutectic	Aladdin, CHN	2.42		126,300	0.271	
	decanoic-caprylic acid (DA-CA) + MWCNT-OH	eutectic		2.45		128,700	0.338	
	decanoic-caprylic acid (DA-CA) + Fe2O3	eutectic		2.51		122,300	0.371	
	decanoic-caprylic acid (DA-CA) + Cu	eutectic		2.43		121,800	0.321	
[61]	decyl alcohol myristyl alcohol (DA-MA) eutectic mixture 87:13	eutectic		3.9		178,200	0.277	
	(DA-MA) eutectic mixture + expanded grapihte (DA-MA/EG) 14:1	eutectic		3.55		172,300	0.942	
[62]	n-dodecane	organic	Aladdin, CHN	-6.41		258,120		
	n-tridecane	organic	Aladdin, CHN	-2.92; -17.52		179,390 (m1); 55,760 (m2)		
	n-tetradecane	organic	Aladdin, CHN	8.92		276,510		
	n-dodecane micro capsules			-8.96		110,530		
	n-tridecane micro capsules			-4.9; -18.19		63,670 (m1); 30,390 (m2)		
	n-tetradecane micro capsules			6.65		116,190		
[63]		inorganic		0		324,350		

Table 1 (*continued*)

Authors	PCM name	Typology	Supplier	Melting Temperature, Tm (°C)	Freezing Temperature, Ts (°C)	Latent heat of phase change, L (J kg⁻¹)	Thermal conductivity, k (W m⁻¹ K⁻¹) solid	liquid
	Water sodium solution polymer (SP) 0.5wt % solution							
[64]	RT5HC	organic	Rubitherm, DE	6	5	250,000	0.2	0.2
[65]	decyl alcohol (DA)	organic	Sinopharm Chemical Reagent Co., Ltd., CHN	5	2.6	205,000	0.162	
	DA + expanded graphite (EG)			1	1.7	185,000	1.854	
	DA/MgO/EG			1.1	2.4	194,600	1.873	
[66]	SSD	inorganic		31.89	12.71	148,200 (m); 55,440 (f)		
	SBCKN	inorganic		8.07	4.2	101,100 (m); 54,590 (f)	0.25	
	SBCKN/EG 5wt%			5.92	5.67	99,350 (m); 66,390 (f)	0.43	
[67]	paraffin	organic		28	26.6	192,000		
	MicroPCMs (paraffin) in PU-based shell. Paraffin 68wt%	organic		27.1	25.6	130,000		
	MicroPCMs (paraffin) in PU-based shell. Paraffin 25wt%	organic		26.8	25.7	50,000		
[68]	PEG400	organic	Sigma-Aldrich Inc.	4.6	-15.3	100,000		
	PEG600	organic	Merck Chemical Ltd.	21	7.7	125,000		
	HNTPEG400 (Hallosyte Nano Tubes)			1.3	-27.8	22,000		
	HNTPEG600 (Hallosyte Nano Tubes			13.9	-8.3	24,000		
[69]	5%D-glucose-NaCl solution	organic		-4.39		259,900	0.5267	
	5%glycine-NaCl solution	organic		-5.94		291,150	0.584	
	5%D-sorbitol-NaCl solution	organic		-4.33		269,700	0.5435	
	*only 5% concentrations are reported here. The authors also investigated 7.5, 10, 12.5, 15% for each PCM typology)							
[70]	1-dodecanol-tetradecane binary eutectic mixture 26.3:73.7 (BEM)	eutectic		3.43	4.17–2.58	213,000		
	BEM/EG 7%wt			3.45	7.02–2.14	195,000	3.206	
[71]	decyl alcohol (DA) – lauryl alcohol (LA)	eutectic		-3.2		179,700	0.2869	
	DA-LA/MWCNT-OH/SDBS 0.15wt%			-3.1		178,400	0.3323	
[72]	Sodium sulfate decahydrate (SSD)	inorganic		23.36	12.56	61,630 (m); 46,600 (f)		
	SSD-BCKN3 (borax 3wt%, CMC 3wt%, KCl 5wt%, NH4Cl 20wt%)	inorganic		6.8	6.1	97,050 (m); 69,000 (f)	0.264	
	SSD + (borax, CMC, KCl, NH4Cl) in diff wt %							
[73]	OP5E (paraffin, PA)	organic	Ruhr Energy Technology, CHN	5–6		240,000	0.2	
	PA/MWCNTs/SDBS (1wt% MWCNT, 2:1 MWCNT:SDBS)			5.5		222,700	0.3723	
[74]	n-tetradecane (TD)	organic		9.78	1.96	208,000		
	PNCT-HXL-TD (foam stable composite PCM, 35wt%)			7.71	0.4	73,000		
	PNCSi-HXL-TD (foam stable composite PCM, 40wt%)			7.52	1	82,500		
[75]	LTPCM water core and ethylcellulose (EC) (Low Temperature PCM Microcapsules)	inorganic		0.3; 7.6	3.5	286,510	0.4655	
[76]	RT5	organic	Rubitherm, DE	5	7	156,000	0.2	0.2
[77]	water	inorganic						
[27]	inorganic salt-water solution	inorganic		-26.7	-30.6	154,400		
[78]	C-18	inorganic	Climsel	-18		306,000	0.6	
	E-21	inorganic	Cristopia	-21		233,000		
[79]	Energain	organic	DuPont					
[80]	inorganic salt-water solution	inorganic		-26.7	-30.6	154,400		
[81]	Microencapsulated n-tetradecane in PU foam, 13.5wt%	organic	Microteklabs, USA	6		24,860	0.03279	
[82]	E-26	eutectic	PCM products Ltd.	-26		260,000	0.58	
[83]	RT27	organic	Rubitherm, DE	27.5		55,000	0.2	
	RT28HC	organic	Rubitherm, DE	28		140,000	0.2	
	RT31	organic	Rubitherm, DE	30.5		24,350	0.2	
	RT35	organic	Rubitherm, DE	32.5		26,000	0.2	
	RT35HC	organic	Rubitherm, DE	35		105,000	0.2	
	RT42	organic	Rubitherm, DE	41		30,000	0.2	
	RT44HC	organic	Rubitherm, DE	43		94,500	0.2	
	RT47	organic	Rubitherm, DE	45		20,000	0.2	
	C48	inorganic	Climsel	46.5		110,000	0.2	
[84]	RT35HC	organic	Rubitherm, DE	35		220,000	0.2	
	RT28HC	organic	Rubitherm, DE	30	27	250,000	0.2	
	RT31	organic	Rubitherm, DE	33	27	165,000	0.2	

(*continued on next page*)

Table 1 (*continued*)

| Authors	PCM name	Typology	Supplier	Melting Temperature, Tm (°C)	Freezing Temperature, Ts (°C)	Latent heat of phase change, L (J kg^{-1})	Thermal conductivity, k (W m^{-1} K^{-1}) solid	liquid
	PT27	organic	PureTemp LLC, USA	27		263,000	0.15	0.25
	PT28	organic	PureTemp LLC, USA	28.1		254,000	0.15	0.25
	PT29	organic	PureTemp LLC, USA	28.6		202,000	0.15	0.25
	A27	organic	Phase Change Materials Products Ltd., UK	27		250,000	0.22	
	A28	organic	Phase Change Materials Products Ltd., UK	28		265,000	0.21	
	A29	organic	Phase Change Materials Products Ltd., UK	29		230,000	0.21	
	A30	organic	Phase Change Materials Products Ltd., UK	30		230,000	0.21	
	A31	organic	Phase Change Materials Products Ltd., UK	31		230,000	0.21	
[28]	C18 Inertek 29	inorganic		18.3	14.2	185,400		
	microencapsulated PCM in PU (C18 Inertek 29), 40wt%			18.1	14	49,000		
	microencapsulated PCM in PU (C18 Inertek 29), 50wt%			18.3	14.3	60,000		
[85]	RT35HC	organic	Rubitherm, DE	35		220,000	0.2	
	RT5HC	organic	Rubitherm, DE	5		240,000	0.2	
[86]	RT18HC	organic	Rubitherm, DE	18		220,000		
[87]	E-26	eutectic	PCM products Ltd.	-26		260,000	0.58	
	E-29	eutectic	PCM products Ltd.	-29		222,000	0.64	
	E-32	eutectic	PCM products Ltd.	-32		243,000	0.56	
[88]	RT3HC	organic	Rubitherm, DE	3		190,000	0.2	
	RT5	organic	Rubitherm, DE	5		180,000	0.2	
	RT8HC	organic	Rubitherm, DE	8		190,000	0.2	
[89]	RT5	organic	Rubitherm, DE	4.96	4.84	180,000	0.2	
[90]	water	inorganic						
[17]	RT2HC	organic	Rubitherm, DE	3	1	200,000	0.2	
	RT4	organic	Rubitherm, DE	5	3	170,000	0.2	
	RT5HC	organic	Rubitherm, DE	6	5	250,000	0.2	
[91]	SP-24	inorganic	Rubitherm, DE	-22	-23	220,000	0.6	
[92]	Acqueous salt solution	inorganic		-10		230,000	2.2	2.2
		inorganic		-33		215,000	0.6	0.6
[93]	OP5E	organic	Ruhr New Material Technology Co., CHN	6	5	235,000	0.2	
[94]	RT0	organic	Rubitherm, DE	0		145,000	0.2	0.2
	RT2HC	organic	Rubitherm, DE	2		170,000	0.2	0.2
	RT3HC	organic	Rubitherm, DE	3		160,000	0.2	0.2
	RT4HC	organic	Rubitherm, DE	4		145,000	0.2	0.2
	RT5HC	organic	Rubitherm, DE	5		220,000	0.2	0.2
	RT8HC	organic	Rubitherm, DE	8		160,000	0.2	0.2
[95]	RT5	organic	Rubitherm, DE	6.46		143,740	0.159	
	RT5-modified (fumed silica + graphene)	organic		6.49		131,860	0.247	
[96]	Tetradecane-Lauryl Alcohol-Expaned graphite	eutectic		4.3		247,100	0.9657	
[97]	SP-50	inorganic	Rubitherm, DE	-52	-48	190,000	0.6	
[98]	Sodium polyacrylate -0.1wt% MWCNT-water			-0.037		335,400	0.9021	
[99]	n-octanoic acid-myristic acid composite	organic		7.1		146,100	0.2832	
	Potassium sorbate-water composite	inorganic		-2.5		256,200		
[100]	Eutectic salt	eutectic	Shanghai Wenkang Co. Ltd, CHN	-80		82,320		
[101]	E-21	eutectic	Cristopia	-21.3		233,000	0.5	
[102]	E-21	eutectic	Cristopia	-21.3		233,000	0.5	
[103]	Sodium chloride, glycerol solution, water	eutectic		-30		175,300		
[104]	water	inorganic		0		334,000		
	Potassium sorbate	inorganic		-2.5		256,000		
	Tetradecane + docosane	organic		2.5		234,000		
	Tetradecane	organic		5		214,000		
[105]	BPCMG: Brine (KCl + NH$_4$Cl) in super absorbent polymer (SAP) gel	eutectic		-21		230,620	0.589	
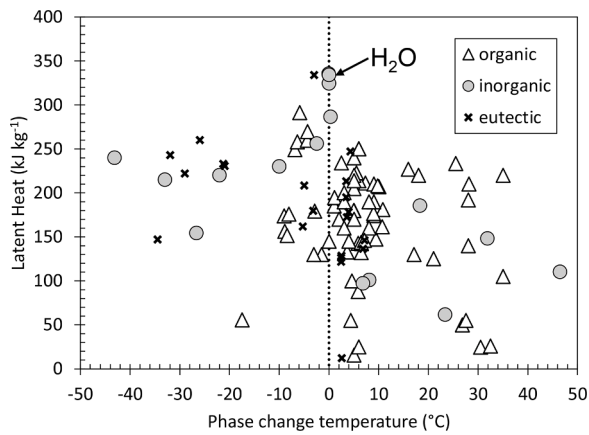
Fig. 3. Latent heat as function of the melting temperature of the PCMs reported in Table 1.

$m^{-1} K^{-1}$, with negligeable reduction of the melting enthalpy. By inserting 0.1 wt.% MWCNTs in a water-sodium solution based PCM, a 19.17% increase in the thermal conductivity was reported [98], reaching the value of 0.90 W $m^{-1} K^{-1}$. The insertion of 1.5wt% silver-titania hybrid nanocomposite into ethyl trans-cinnamate (6.8 °C melting temperature) led to 52% of thermal conductivity augmentation (figuring out at 0.54 W $m^{-1} K^{-1}$). Besides, the immersion of metal foams in PCMs have been proposed to enhance the thermal conductivity. For example, Xiao et al. [107] by immersing copper foam in paraffin obtained a 15 times thermal conductivity increase. By obtaining microcapsules consisting of 50wt% calcium carbonate ($CaCO_3$) shell and n-octadecane PCM, Yu et al. [108] reported a significant thermal conductivity improvement of about 725% compared with pure PCM, reaching 1.26 W $m^{-1} K^{-1}$. For additional survey works, the reader may refer to Nie et al. [35]. Foam-fin combinations were tested by Liu et al. [109]
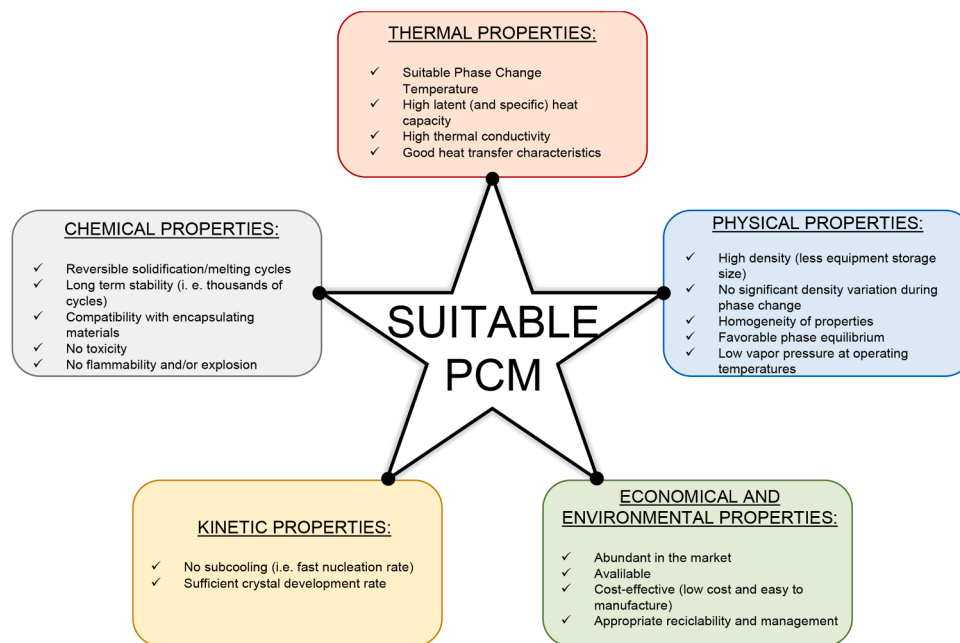
Fig. 4. Selection criteria for the suitable PCM. Adapted from [38].

Fig. 5. Advantages (PROs) and disadvantages (CONs) of PCM classified by chemical composition.

3.2. Subcooling

The subcooling phenomenon may occur during the solidification process. It implies the need of cooling the PCM at a temperature lower than its freezing point to let the solidification process start, which results in a loss in system efficiency. Once the process is triggered, the PCM temperature jumps to the nominal phase change temperature and the solidification continues as expected. This phenomenon can be ascribable to a low rate of nucleation or a slow rate of nuclei growth [110]. As reported in Fig. 5, the subcooling effect is particularly significant for inorganic PCMs, whilst almost negligeable for organic ones. Aiming at overcoming the subcooling issue, the addition of nucleating agents has demonstrated to be an effective solution. Zhang et al. [111] let the degree of subcooling drop from 14.5 K to 0.8 K by employing SiO_2 nanoparticles into PCM-in-water emulsion. Wang et al. [112] added 2 wt.% of graphene nanoparticles to OP10E in water to drop the subcooling of the PCM from 9.9 K to 0 K.

3.3. Phase segregation

The phase segregation occurs when two or more phases constituting the PCM can be noticed, separately, after a complete phase change process. This phenomenon is significantly evident for inorganic salt hydrates PCM [33]. This problem may be overcome using thickening agents or gelling [113]. The former increases the viscosity of the PCM whilst its melting point remains almost the same. The gelling agents inhibit the phase separation by forming a 3D matrix inside the PCM. However, the heat capacity is negatively affected by the addition of thickening agents [114]. Cabeza et al. [115] reported heat capacity reductions of up to 35%.

3.4. Leakage

The PCM leakage is preeminently due to the volume expansion occurring during the transition from solid to liquid. As reported by Nie et al. [35], the PCM should be entrapped in container through microencapsulation or be immersed in a matrix. Since the microencapsulation is still not a cost-effective technique and due to the difficulties facing during the process of selecting and designing the appropriate material in accordance with the application, the addition of matrix has been adopted as a feasible mean to prevent leakage. By immersing capric-nonanoic acid mixture (6.84 °C melting point) into a 90 wt.% expanded graphite matrix, leakage was inhibited by Wang et al. [116]. In general, polymeric matrixes require up to 30 wt.% whilst ceramic ones up to 70% to eliminate the leakage to occur [35]. Additional reviewed works on leakage prevention can be found in [35].

3.5. Long-term stability

The long-term stability of the thermo-physical PCMs properties is essential for their use in a real application. Therefore, several authors have analyzed the PCM stability after a certain number of melting-solidification cycles. Xu et al. [98] evaluated the step cooling curve of water and 1 vol.% sodium polyacrylate PCM at the beginning and after 100 cycles. It was found that the two curves mostly overlap, suggesting

good stability. The authors, also, calculated, through a differential scanning calorimeter, the latent heat value after 100 cycles obtaining negligeable differences. Nie et al. [95] developed a new composite phase change material for a portable box for cold chain applications. The composite PCM consisted of the paraffin RT5, with the addition of fumed silica and graphene. The authors investigated the cyclability of the pure and composite PCMs, finding that the two PCMs presented good thermal stability, as reported in Table 2.

3.6. Corrosion

The preliminary evaluation of the corrosive effect of the PCM on the construction material is essential to design a latent thermal storage system. As stated by Nie et al. [35], several studies on the effects of salt solutions and eutectic-based ones for low temperature application on different metals have been carried out. However, no definitive solutions in overcoming the corrosion have been achieved. Orò et al. [117] investigated the compatibility of PCM (from -21 °C to 15.4 °C melting temperature) with different metals (copper, aluminum, stainless steel 316 (SS316), and carbon steel) and four polymers to find the most appropriate container. By focusing only on metallic materials, SS316 is considered the most suitable for a cold storage application. An interesting work was conducted by Ferrer et al. [118]. Five specimens of different material (aluminum, SS316, SS304, carbon steel, and copper) and four different PCMs (inorganic mixture, ester, two fatty acid eutectics) were used. It was reported that aluminum is suitable for the ester and for the eutectic PCMs, whilst SS316 and SS314 can be adopted for all kinds of PCM. The corrosion test was also conducted by Farrell et al. [119] who analyzed PlusICE E17 (17 °C melting temperature) and Climsel C18 (18 °C melting temperature) on copper, aluminum, and copper-aluminum alloy materials. Significant mass losses were detected for the copper sample, whilst no mass loss was found for the alloyed sample. The design with aluminum performed well for E17.

3.7. Health, environmental and economic aspects

A complete review on the toxicity evaluation and health hazards of different types of PCMs has been proposed by Chandel and Agarwal [120].

In Fig. 6, the main results obtained in [120] are summarized. As seen, different impacts on the human health and environment safety may derive from different kinds of PCMs. Among the organic ones, it has been observed that vegetable oils are safer than paraffins, and they can also be considered a green technology due to their environmental sustainability. However, they generally have melting points that cannot match cold storage application requirements [120], though some exceptions can be found in the market (CrodaTherm 9.5 [121]). Fatty acids present a remarkable odor which limits their exploitation. Salt hydrates can be hazardous with reported issues such as eye irritation and asthma.

To conduct a comparative analysis of the environmental impacts of an already existing technology versus an innovative LTES one, a Life Cycle Assessment (LCA), in accordance with the International Standard ISO 14,040 [122], is necessary. As reported in David et al. [123], after having defined the goal and scope of the analysis, the inventory analysis, life cycle impact assessment and interpretation phase are followed. It is

Table 2
Thermo-physical properties of PCM after 0–100–200 cycles [95].

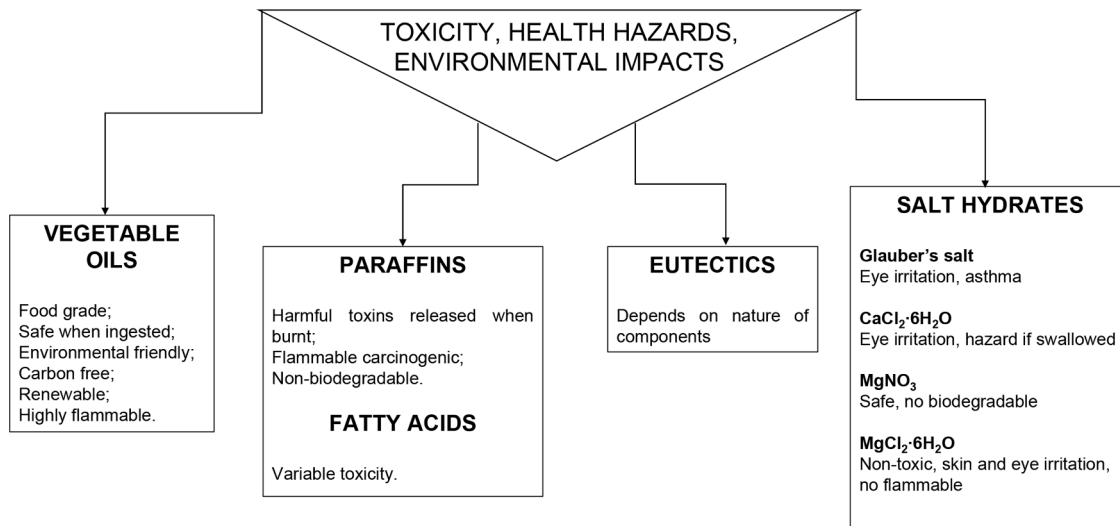| Sample	Cycles	Melting Temperature (°C)	Freezing Temperature (°C)	Latent Heat (kJ kg⁻¹)	Supercooling degree (K)
Pure PCM	0	6.46	2.82	143.74	3.64
	100	6.54	2.41	142.67	4.13
	200	6.57	2.57	141.50	4.00
Composite PCM	0	6.49	3.26	131.86	3.23
	100	6.57	3.17	130.72	3.40
	200	6.65	3.11	128.99	3.43

Fig. 6. Toxicity, health hazards and environmental impacts of different PCMs.

required the evaluation of the environmental impacts by considering the application in its complexity. Therefore, the needed energy and materials, transport means, maintenance, and disposal (re-use) must be taken into consideration.

The goal and scope definition phase involves the clearly statement of what it is wanted to demonstrate by performing the LCA. At this stage, the system boundaries, the functional units, and which categories have impacts on the analysis must be declared and clarified. The inventory phase prescribes the analysis of all the required input data (energy, materials) and it returns outputs in terms of the amount of solid, liquid, gas released into the environment. During the impact assessment phase, the data coming from the precedent stage are converted into damage indicators. Finally, all the results are analyzed during the interpretation phase, and this lets to make the final decision. In Fig. 7, the scheme of a LCA for a building PCM-based application is shown.

In parallel with the evaluation of the environmental consequences of the adoption of a latent thermal storage, a Life Cycle Cost Analysis [125] is needed. In particular, the analysis prescribes the estimation of agency, user, and environmental costs. The agency costs are related to the necessity of finding an intermediary who can solve problems associated to conflicts of interest, conflicts of relation between stakeholders or management problems. The user cost concerns the use of a fixed capital

asset, which is the loss in the asset's value due to its use. Finally, environmental costs are intended to represent the potential deterioration of natural assets due to economic activities.

4. Refrigerated transport along the cold chain

As Fig. 8 indicates, a typical cold chain consists of different activities (usually in series) that ensure the temperature control for the safe management of perishable products. It involves, essentially, the products harvesting, storage, and transportation. The latter is particularly significant because it plays a fundamental role during the very diverse steps along the supply chain.

To achieve the goal of maintaining the correct temperature at different stages, diverse typologies of transport can be found: there can be inland transportation, very long-distance or intercontinental transport involving air, sea or rail transportations, or city logistics for a short-haul distribution.

It is clear that different modalities deal with different costs and environmental impacts. Therefore, the sustainability and carbon footprint are two aspects that must be deeply taken into consideration for the choice of the most suitable means of transportation.

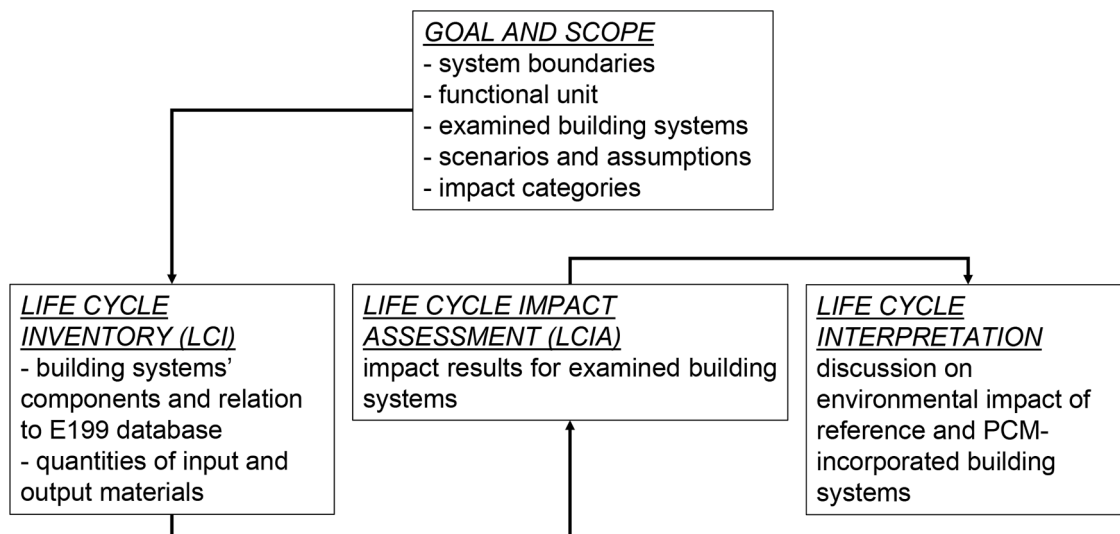In Table 3, the carbon emission and cost of the typologies of transport

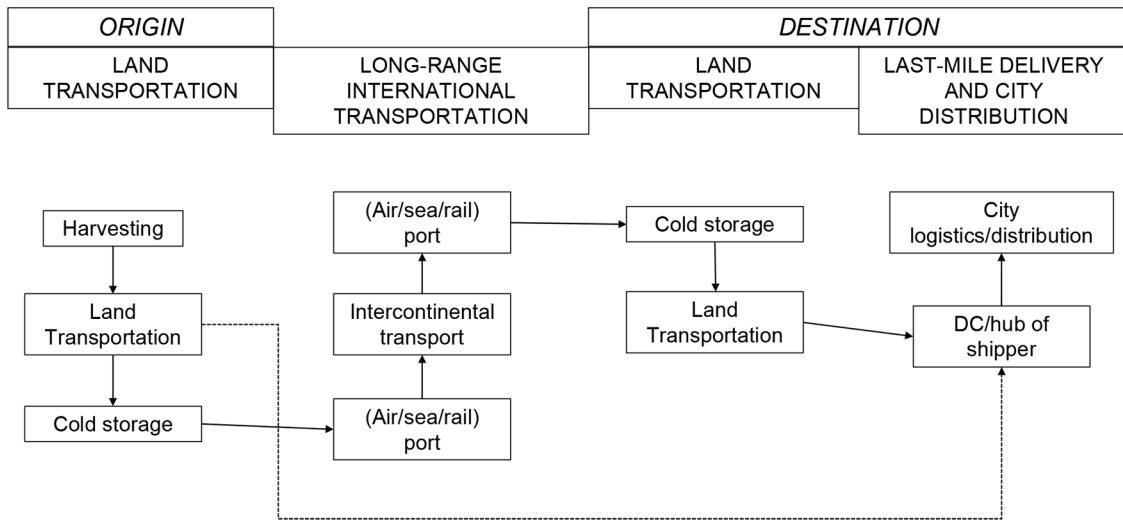**Fig. 7.** LCA for a building PCM-based application. Adapted from [124].

ORIGIN		DESTINATION	
LAND TRANSPORTATION	LONG-RANGE INTERNATIONAL TRANSPORTATION	LAND TRANSPORTATION	LAST-MILE DELIVERY AND CITY DISTRIBUTION

Fig. 8. Cold chain stages. Adapted from [126].

Table 3
Emission and costs of different transport modalities [126].

Transport typology	Emission (gCO$_2$ ton^{-1} km^{-1})	Cost ($ ton^{-1} km^{-1})
Sea Transport	3 (container), 0.6 (bulk)	0.01 (dry cargo) to 0.025 (reefer)
Air Transport	218 (short-haul), 159 (long-haul)	0.8–1.5
Inland waterways	50.62	0.09
Rail	139.8	0.2
Truck	15.6	0.12

composing the cold chain are shown.

Since the main focus of this work is on the road transportation, no additional details on the other transport methods will be given.

The road transport is the most adopted way for inland freight transport [126]. In 2013, 75% of the entire freight transported along the European countries involved road transport [126]. Moreover, this number can reach 95% if considering only agri-food transportation. As stated by Tassou et al. [31], primary, secondary, and tertiary distribution can be detected. The primary distribution involves the transport from the food factory to the regional distribution centers and it is mainly served by large articulated vehicles (up to 44 ton). This transport method is also used for secondary distribution, that is from regional distribution centers to shops. Finally, rigid vehicles (up to 32 ton) are employed for tertiary distribution (to small shops).

The international carriage of perishable food products is regulated by the international ATP agreement [30] which aims at setting rules and standards for the temperature-controlled means of transport. In the next section, details of the ATP agreement will be enucleated.

4.1. ATP agreement

The insulated equipment of a transport vehicle consists of rigid insulating walls or doors which limit the heat transfer between the external environment and the refrigerated cell. If a transport mean is *isotherme normal* I$_N$, normally insulated equipment, its global heat transfer coefficient K (W m^{-2} K^{-1}), defined as the ratio between the heat flow and the temperature difference between inner and outer vehicle body and the heat transfer surface areas, should not be greater than 0.70 W m^{-2} K^{-1}. On the contrary, an *isotherme renforcè* vehicle I$_R$, heavily insulated equipment, should have a K value less than or equal to 0.4 W m^{-2} K^{-1}. Moreover, if the width of the transport equipment exceeds 2.5 m, the insulation wall thickness cannot be thinner than 45 mm. The need

of an I$_R$ or I$_N$ vehicle depends on the nature of the transported goods (if frozen, chilled, positive temperature).

The equipment can also be subdivided into *refrigerated* or *mechanically refrigerated* ones. The former deals with all the transport means which adopt a cold source to maintain the temperature inside the cell at a suitable level, with an average outside temperature of 30 °C. They can be of class A, if the temperature inside the vehicle body is lower than 7 °C, class B if lower than -10 °C, class C if lower than -20 °C, and class D if lower than 0 °C. For what stated above, it is clear that classes B and C must be of I$_R$ type ($K \leq 0.4$ W m^{-2} K^{-1}). The mechanically refrigerated equipment, instead, concern all the transport means which use a refrigeration system (an own one or served jointly with other units of transport equipment by such an appliance). They are classified into 6 different classes (from A to F) depending on their ability in ensuring a desired temperature value inside the refrigerated body (T_i) with an external temperature of 30 °C:

- Class A: 0 °C $\leq T_i \leq$ 12 °C
- Class B: -10 °C $\leq T_i \leq$ 12 °C, $K \leq 0.4$ W m^{-2} K^{-1}
- Class C: -20 °C $\leq T_i \leq$ 12 °C, $K \leq 0.4$ W m^{-2} K^{-1}
- Class D: $T_i \leq$ 0 °C
- Class E: $T_i \leq$ -10 °C, $K \leq 0.4$ W m^{-2} K^{-1}
- Class F: $T_i \leq$ -20 °C, $K \leq 0.4$ W m^{-2} K^{-1}

Other classifications are related with *heated* and *refrigerated and heated* equipment [30].

The ATP standard also gives provisions on how to check the status of the different equipment for compliance with the standards [30]. The equipment conformity should be checked before starting its service, periodically (at least 2 times per year) and when required by the competence authority. The check the insulation capacity of the equipment when in service consists of an inspection to establish the durability stated by the manufacturer, the general design of the insulating envelope, the method as to how the insulation has been applied, the condition and the thickness of the walls, and the condition of the insulated compartment. Experts may also require additional documents.

The test to confirm the validity of the refrigeration equipment results in the issue of a valid ATP capacity report. Note that considering the temperature limit imposed by the specific class and the corresponding heat flow Q to be extracted to ensure the limit when an external temperature of 30 °C is fixed, 1.35 times Q is required to endorse the refrigeration equipment installed on a refrigerated vehicle. If, instead, the refrigeration equipment is tested alone, it should provide a cooling capacity 1.75 times higher than the calculated Q in order to receive the

ATP certificate. The ATP certificate covers both the insulation body and the refrigeration equipment.

4.2. Refrigerated vehicles overview

Depending on what cold chain stages the refrigerated transport is involved in, different solutions can be adopted (containers, trailers, semi-trailers, trucks, vans [31]). The refrigerated vehicles are about 4 million. The market share consists of 55% of vans, 25% of semi-trailers and 20% of trucks [2].

It must be stressed that diverse sizes of the insulation and refrigeration equipment of the refrigerated vehicle, result in specific performance, energy/fuel need and pollutant emissions, consequently.

4.2.1. Wall insulation

As reported in [127], when dealing with the design factors affecting the insulation design, despite of the specific typology of the refrigerated vehicle, the subsequent points must be taken into consideration:

- *Exterior conditions*: the extreme outer temperature, relative humidity, solar effect and wind effect.
- *Targeted interior conditions*: psychrometric variables (temperature and relative humidity).
- *Insulation materials properties*: moisture permeability, moisture retention, heat transfer properties, chemical and physical stability, structural limit, economical aspect.
- *Infiltration*: air and moisture due to door openings or cruising speed.
- *Trade-off between* operating requirements and designing cost.
- *Construction constraints*: exterior dimensions and minimum tare weight imposed by regulation or international agreement; for traditional European semi-trailer rigid box the external dimensions are 13.56 m x 2.6 m x 2.75 m (length, width, height) [31];
- *Others*: accidents or shock during the travel which can potentially deteriorate insulation ability.

Regarding the insulation wall thickness, trailers and trucks usually require 25 to 65 mm foam insulation material (Poly-Urethane foam, $k = 0.022$ W m^{-1} K^{-1}) when carrying fresh cargos, or 35 to 100 mm when dealing with frozen ones [127]. By considering 2 traditional europallets (1000 mm x 1200 mm) inserted side by side, it can be deduced that the thickness results in a numerical value, in most of the cases, no higher than 45–50 mm [31]. PU-foam is preferred due to its intrinsic hydrophilicity and relative low cost, with contemporary good mechanical properties [127]. A metal sheet is usually adopted for the exterior insulation wall surfaces of the vehicle in order to prevent air and moisture infiltration. On the other side, vapor barriers wrap the interior insulation of body surfaces. The inner layer presents protections against pallet-trucks and forklifts during loading/unloading operations. A typical material suitable to act as vapor barrier can be the aluminum foil, properly sealed at joints [127]. As reported in different works [31,79] the insulation foam aging is an important factor to be considered as it significantly impacts the thermal performance of the insulation material. On average, a typical value of 5% per year for loss in insulation capacity is reported. More specifically, between 3% to 5% annual increase in thermal conductivity of the insulator has been observed [31]. That is, an increase of 55% in energy consumption (and carbon dioxide emissions, consequently) after nine years of operation. Besides the manufacturing process can affect the insulation performance of the insulation wall, mainly by affecting the global heat transfer coefficient K through the wall. K values from 0.82 to 1.24 W m^{-2} K^{-1} have been observed in [128] for similar refrigerated vans.

4.2.2. Refrigeration equipment

Depending on the way energy is supplied to the refrigerated equipment, two categories can be identified: *self-powered systems* usually adopted for large size vehicles (trucks, trailers) and *vehicle-powered*

systems (typically for vans or small trucks) [127]. In either case, the cooling unit relies on vapor compression technology.

When dealing with self-powered refrigeration systems, four other sub-categories can be listed. The first involves the adoption of an own heat engine for the mechanical power, i.e. an autonomous unit from the vehicle. Open-shaft compressor is connected to the engine while fans and blowers are triggered by a belt-and-pulley system [127]. In such a system, the cooling capacity modulation can be achieved either by a specific control of the speed or by switching the engine on and off. The second sub-category include the systems which require electrical power to operate. The compressor, condenser, evaporator fans motors are fed by an engine-driven generator. The advantage of adopting an electrical system is the possibility of limiting the losses due to belt transmission. The trailer refrigeration systems present the cooling unit which is usually mounted on the top, with the evaporator and fans facing the inside of the refrigerated body. The entire system consists of a diesel engine connected to a battery-charging alternator while mechanically and/or electrically driven systems are also existing. The self-powered large truck systems are very similar to trailer ones. To reduce the polluting emissions particle filters and catalysts can be used [127].

Focusing on vehicle-powered systems two main sub-categories can be identified: the vehicle alternator unit system and direct belt one [31]. These categories are usually related to small trucks or vans. With the former, the electrical alternator is driven by a belt. The alternator feeds the all-electric-vehicle-powered system and is driven either by either the crankshaft or the engine power take-off. To regulate the change in the engine speed, a static converter may be adopted, which maintains a constant direct current voltage [127]. The other vehicle-powered transport means for local delivery of refrigerated products relies on the engine using a belt and pulley system. All other refrigeration components are electrically driven. One of the main disadvantages of adopting such a system is that the performance is strictly related to the vehicle engine's speed, independent from the cooling capacity needs.

As already stated, different refrigeration technologies deal with different transport means which, in turns, are linked to different carbon dioxide emissions. A comprehensive work on CO_2 emission per carried pallets per kilometers of several refrigerated road transport vehicles was assessed by Tassou et al. [31], by discriminating between chilled or frozen carried foodstuffs, single- or multi-drop, and multi-temperature, as reported in Table 4. It must be highlighted that emissions for refrigerant leakage are not considered here.

4.3. How to improve the refrigerated transport sustainability

As affirmed by Behdani et al. [126] the transport cold chain sustainability improvement could be achieved by pursuing two different goals: the enhancement of energy consumption (and, the minimization of the emissions, consequently) of the different refrigerated vehicles or improving the logistics processes.

For the efficiency enhancement of the distribution in global networks, different ICT technologies have been proposed [126]. Focusing on the first goal, and, more specifically on the reduction of pollutant emissions, Lee et al. [129] demonstrated that 42–61% less GHGs were generated by an electric truck compared with a traditional diesel-driven one. In particular, if considering the frequent stops and low average speed scenario, energy consumption reductions of 32–54% were achieved. Nevertheless, for a city-suburban scenario (less stops, higher velocities), the energy consumption was reduced from 5 to 34% and, consequently, GHGs emissions dropped from 19 to 43%. The translation to full electric transport means seems a promising solution even if some drawbacks have firstly to be overcome, such as batteries-life duration, charging points and cost of technology. As reported by Tassou et al. [31], cryogenic cooling systems and eutectic systems may improve the environmental sustainability of refrigerated transport. Phase Change Materials, as already stated in the introductive section, have been attracting more and more attention to be employed as a more sustainable

Table 4

CO_2 emissions (gCO_2 pallet^{-1} km^{-1}) for different refrigerated vehicles [31].

Vehicle	No Ref.	Chilled (single-drop)	Chilled (multi-drop)	Frozen, multi-temperature (single-drop)	Frozen, multi-temperature (multi-drop)
Medium rigid	88	106	109	112	115
Large rigid	85	102	105	108	111
City articulated	56	69	70	73	75
32 ton articulated	51	61	63	65	67
38 ton articulated	48	58	59	61	63
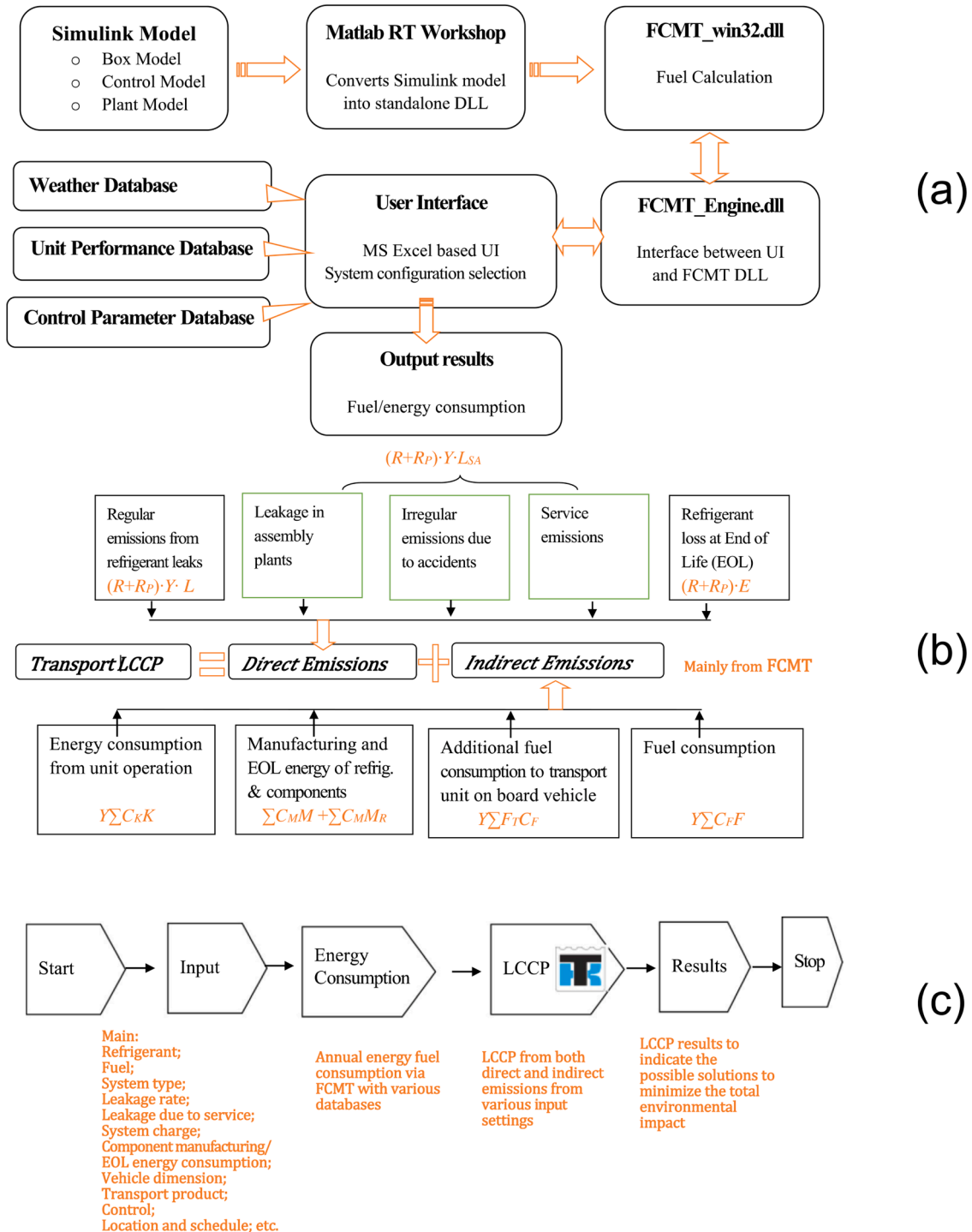
Fig. 9. (a) Thermo King Fuel Simulator, (b) Transport LCCP, (c) Transport LCCP flowchart. Adapted from [32].

alternative in refrigerated transport. In the next section, a detailed and comprehensive review of the PCM integration in refrigerated vehicles will be presented.

Regardless of the refrigerated transportation system, several procedures may be followed, and different performance indicators may be defined and adopted to evaluate the environmental impact [32]. In details, three approaches are fully described [32]: the Total Equivalent Warming Impact (TEWI), the Life Cycle Assessment (LCA) and the Life Cycle Climate Performance (LCCP). The different approaches, however, lead to an estimation for the direct and indirect emissions. Nevertheless, as stated by Li et al. [32] due to the extremely different operating conditions a refrigeration system may face, the LCCP is more trustable and meaningful to estimate the environmental performance impact (and can potentially reduce it). Moreover, knowing the energy consumption inputs, LCA and LCCP approach should result in the same solution, if the focus in only on greenhouse gas emissions.

Therefore, the key points of the transport LCCP calculation procedure developed and proposed in [32] are here reported. The present authors consider this methodology to be used as reference for further analysis to create a new transport LCCP model for every specific refrigerated transport application by following a similar approach.

Before starting the LCCP calculation, the procedure described in [32], prescribes to estimate the energy/fuel consumption by the adoption of the Thermo King Fuel Simulator (Fig. 9(a)). To address this goal, a Simulink model in Matlab environment is developed. In particular, as shown in Fig. 9(a), it consists of a "Box Model" which lets to obtain the necessary cooling load to maintain the system at a determined temperature. At this level, some input data are needed, such as box dimension, the material property for the insulation layer and ambient as well as the box temperature. An intermediate result is the evaluation of the heat losses through the box. The solar radiation and door openings can also be taken into account. As a subsequent step, there is the "Control Model" which deals with the control of the engine speed, fan speed, and refrigeration capacity, consequently. Finally, strictly connected to the control model, the "Plant Model" can be found which predicts the system energy efficiency due to those particular conditions. Once the energy/fuel consumption response is obtained, the proposed transport LCCP calculation can be assessed, as depicted in Fig. 9(b). One can now estimate the direct and indirect emissions of the refrigeration system, by adopting the following equation (Eq. (1)) [32]:

$$TransportLCCP = (R + R_p)\{Y(L + L_{sa}) + E\} + Y\sum(C_f F + C_k K) + Y$$
$$\times \sum F_t C_f + \sum C_m M + \sum C_m M_r$$

(1)

In Fig. 10(b) the physical explanation of each term can be appreciated. For the sake of brevity, details are not provided here as they can be found in [32]; a flowchart is presented in Fig. 10(c) instead.
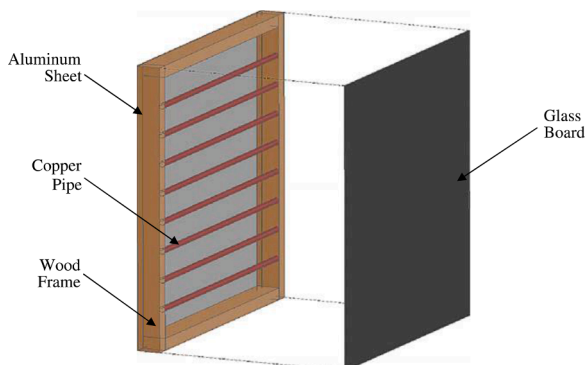

Fig. 10. New PCM-based insulation wall [76].

5. PCMs in refrigerated transport applications

In this section, the works involving the adoption of PCM for innovative refrigerated transport applications are explained in detail (Table 5).

In particular, from the reviewed works, three different approaches have been identified and critically discussed.

The first one regards the enhancement of the insulation wall by the insertion directly into the insulation material or the employment of PCMs in proximity of the insulation layer. The second one relates to the application of PCM in the refrigeration unit which can be alternatively set inside or outside the refrigerated space, and the last one involves the use of eutectic plates.

The effect of other parameters affecting the heat transfer performance have also been analyzed, such as the presence of the food load, the external temperature, and the door openings. Whether the latent thermal energy storage systems were designed to act as an active or passive cooling source, or if the new system required an additional active refrigeration unit have also been highlighted.

5.1. PCM in the insulation wall

A pioneering study on the effect of the integration of the PCM inside the insulation wall of a traditional refrigerated truck was conducted by Ahmed et al. [76].

As depicted in Fig. 10, the authors developed an in-house-made insulation wall by inserting eight copper pipes consisting of PCM into an 8.89 cm traditional polyurethane foam layer. By means of a computer program simulating the real operations, the paraffin-based RT5 PCM having a melting temperature at around 7 °C and with a latent heat value of 156 kJ kg^{-1} was selected to be the most suitable option. The authors considered the refrigerated cell to be set at a temperature close to 4 °C. Different operating conditions were studied such as a single-day operation and month-long one. The values of external temperature, relative humidity, wind and pressure information were acquired and stored by a weather station connected to a computer. The incident solar radiation was also monitored and recorded. To evaluate the effectiveness of the newly-developed insulation wall, two identical small rooms of 1.22 m x 1.22 m x 1.22 m were constructed aiming at simulating a truck trailer refrigerated cell. One room (defined by the authors "Control Unit") made of the traditional insulation, i.e. without PCM, whilst the other (the "PCM Unit") equipped with the new PCM-based walls. An active system consisted of a heat exchanger inside each room linked to a unique external chiller was developed to ensure the internal temperature to be maintained at a target value of 4 °C. For the single-day operation scenario interesting results were obtained. For what concerns the heat flux transmitted through the insulation walls, remarkable reductions were obtained for the southern, eastern, and top surfaces (from 29.7% to 42.4%) and both reduction and delay of the peak heat transfer. By considering the entire room, a global reduction of 18.3% in heat flux was calculated which resulted in a 12.3% reduction in the transmitted heat. Similar results were reported when considering the month-long operation scenario, that is 29.1% heat flux reduction, and 16.3% reduction in the heat entering the room. The PCM-based system lowered the temperature swing, and this can be potentially beneficial for the operating life of the cooling unit. Positive impacts can also be related to energy conservation and less emissions from the diesel-driven refrigeration unit of a standard refrigerated truck.

Glouannec et al. [79] also conducted experimental and numerical investigations of the heat transferred through a novel insulated PCM-based insulation panel for vans. The authors developed an 86 cm tall and 16.2 cm long insulation layer. The insulation wall consisted of an external body (0.1 cm), an air gap of 10 cm, a fiberglass of 0.1 cm, a poly-urethane foam layer of 5.8 cm and the inner face made of 0.2 cm of Polyester+fiberglass. To that wall, adopted as reference case, 1 cm of aerogel and 0.2 cm of reflective multi-foil (RMF) were added to

The figure labels in Fig. 10 read: Aluminum Sheet, Copper Pipe, Wood Frame, Glass Board.

Table 5

Works regarding PCM integration into refrigerated transport applications.

Authors	PCM (Melt/Solid Temperature (°C))	PCM location	Vehicle	Type of products	Product load (Y/N)	Exp/Num	Active (A) /Passive (P) cooling	Temp ext	Door opening (Y/N)	Economic analysis (Y/N)	Savings (Compared with no PCM)
[76]	RT5 (5/7)	Insulation wall	Truck	Food, positive temperature Temp target inside cell: 4 °C	N	E	A	Profile	N	N	*Single day* avg -18.3% of Heat Flux (W/m²) avg -12.3% of Heat Flows (kWh) *Monthly* avg -29.1% of Heat Flux avg -16.3% of Heat Flow
[79]	Energain (21/16)	Insulation wall	Van	Refrigerated products Temp target inside cell: 0 °C	N	E + N	A	10 °C, 30 °C	N	N	Day-time (4 h at 30 °C): -25% energy consumption
[1]	n-tetradecane (6)	Insulation wall	Generic	Perishable products	N	E	–	-1000 W	N	N	In PU-PCM foams, the temperature increase is slower than only PU
[83]	RT27 (27.5), RT28HC (28), RT31 (30.5), RT35 (32.5), RT35HC (35), RT42 (41), RT44HC (43), RT47 (45), C48 (46.5)	Insulation wall	Container	Chilled food Temp target inside cell: 0 °C	N	E	A	Profile (UNI 10349) Solar radiation (UNI 10349)	N	N	max heat peak load reduction: -20.87% max delay in peak: 3 h max energy rate reduction: -4.74%
[84]	RT35HC (35)	Insulation wall	Container	Chilled foods Temp target inside cell: 0 °C	N	E + N	A	Indoor: 19 °C diff ext-int Indoor: solar lamp 1000 W/m² Outdoor: profile	N	N	*Indoor:* 1–2 °C reduced internal surface *Outdoor:* max reduction peak heat transfer rate 8.57%, max peak delay 4:30 *Numerical:* peak heat load reduction: 20%, total energy reduction: 4.7%
[28]	C18 Inertek 29 (18)	Insulation wall	Generic	Food, positive temperature Temp target inside cell: 2 °C	N	E + N	A	Profile: 10 °C to 30 2 h, 30 4 h, 30 to 10 2h	N	N	Energy transferred to the cold space max reduction: 4%
[17]	RT2HC (2), RT4 (4), RT5HC (5)	Insulation wall	Truck	Perishable products Temp target inside cell: 2 to 8 °C	N	N	P	Profile	N	N	–
[92]	SP-24 (-24)	Insulationwall	Truck	Frozen food	N	E + N	P (num)	Exp: 22 °C	N	N	*Exp:* 1 wall containing 6 mm of PCM let

(continued on next page)

Table 5 (*continued*)

Authors	PCM (Melt/Solid Temperature (°C))	PCM location	Vehicle	Type of products	Product load (Y/N)	Exp/Num	Active (A)/Passive (P) cooling	Temp ext	Door opening (Y/N)	Economic analysis (Y/N)	Savings (Compared with no PCM)
								Num: 30 °C			the air in refr space to reach 12 °C about 6 h later than reference. 10 mm, about 40 h *Num:* in truck refr space, temp maintained at -22 °C for more than 20 h
[85]	RT28HC (28), RT31 (31), PT27 (27), PT28 (28), PT29 (29), A27 (27), A28 (28), A29 (29), A30 (30), A31(31)	Insulation wall	Semi-Trailer	Frozen food Temp cell: -10 °C	N	N	A	Profile: from 27 to 31 °C	N	Y	Up to 34.4% refrigeration loads reduction Benefit cost-ratio above 1 Payback time < 3 years Greenhouse gas emission savings of more than 2700 kgCO$_2$/year.
[77]	Water (0)	Cold Storage Unit(CSU) in refr space	Truck	–	N	E	P	–	N	N	–
[27]	Inorganic salt acqueous solution (-26.7/-30.6)	Phase Change Termal Storage Unit (PCTSU) outside refr space	Truck	Frozen food (meat and fishery) Temp target inside cell: -18 °C	N	E	P	30 °C	N	Y	up to 86.4% cost reduction, if the charging process is completed during the off-peak period, and COP refr unit = 1.5
[78]	Climsel C-18 (-18) Cristopia E-21 (-21)	Thin container in refr space	Van	Frozen food	Y About 40 kg of M-packs	E	P	25 °C	N	N	*No-food load scenario*: C-18 let the air to be lower than 0 °C for 6.5 h, E-21 for 8 h, no PCM 1.5 h *food load scenario*: C-18 let the air to be lower than 0 °C for 15.6 h, E-21 for 21.5 h, no PCM 11.5 h
[80]	Inorganic salt acqueous solution (-26.7/-30.6)	Phase Change Termal Storage Unit (PCTSU) outside refr space	Van, Truck, Trailer	Frozen food (meat and fishery) Temp target inside cell: -18 °C	N	N	P	Profile	Y 36 s (30+6), every 30 min. 0–10–20 door openings	N	
[86]	RT5HC (5)	PCM air heat exchanger, inside refr room	Generic	Perishable products Temp target	N	E	A	32 °C	N	N	Power consumption reduction: 16%, on/off

Table 5 (*continued*)

Authors	PCM (Melt/Solid Temperature (°C))	PCM location	Vehicle	Type of products	Product load (Y/N)	Exp/Num	Active (A)/Passive (P) cooling	Temp ext	Door opening (Y/N)	Economic analysis (Y/N)	Savings (Compared with no PCM)
				inside cell: 0–8 °C							compressor cycles: 6 against 13
[89]	RT3HC (3), RT5HC (5), RT8 (8)	Baffle type panels, inside refr room	Truck	Perishable products	N	N	A	Profile	Y 10 cycles (60 min close, 15 min open)	N	Max reduction in energy consumption during opening-door period: 61% (RT3HC)
[90]	RT5 (4.96)	cold TES plates, inside refr space	Container	Perishable products (fruit, veget)	Y	E	P	Profile (13 to 35 °C)	Y 1 time	Y	Energy consumption reduction: 86.7%, operating cost reduction: 91.6%, emission reduction: 78.5%
[104]	Sodium chloride, glycerol solution, water	PCCSU (phase change cold storage unit), Inside refr space	Truck	Frozen products	N	E + N	P	Profile (avg 29 °C)	Y (10 door openings per day)	Y	Energy cost reduction: From 15.4 to 91.43%
[91]	Water (0)	MCU (mobile air cooling unit), inside refr space	Truck	Fresh food	N	E	P	27 °C	N	N	–
[82]	E-26 (-26)	Eutectic plates	Container	Fresh and frozen foods	N	N	P	–	N	N	–
[88]	E-26 (-26), E-29 (-29), E-32 (-32)	Eutectic plates	Truck	Frozen food	N	E	P	Profile	N	N	–
[131]	not specified (-18)	Eutectic plates	Truck	agricultural products	N	N	P	25 °C	N	N	–
[132]	Generic (-29)	EutecticPlates	Truck	Frozen food Temp target inside : -20 °C	Y	N	P	20 °C	Y 60 s	N	–
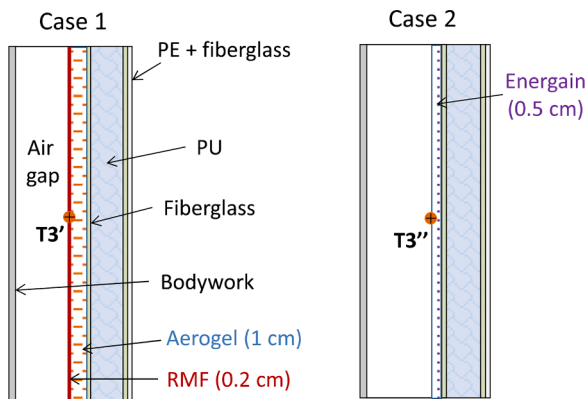
Fig. 11. New designed insulation walls, with Aerogel+RMF (case 1), with Energain (Case 2) [79].

investigate the "Case 1″. Moreover, to the reference case, 0.5 cm of Energain layer was added to analyze the effect of PCM integration inside the insulation layer ("Case 2″), as shown in Fig. 11.

The reference layer and the ones equipped with RMF or PCM layer were used, alternately, as a wall of an insulated small enclosure (0.5 cm³) put inside a climate chamber. This latter was set at the external temperature (10 °C or 30 °C, depending on night and day scenarios, respectively) while an active refrigeration system assured the cooling inside the insulated enclosure to maintain the temperature at 0 °C. The authors calculated the heat flux densities for the first 4 h when the temperature of the chamber was fixed at 10 °C (i. e. simulating the night scenario) and for the next 4 h when temperature was set to 30 °C. A reduction of 36% of the consumed energy for the case 1 was obtained. Besides, the PCM reduced the energy consumption by 25% compared with the base case. In case 1, the authors also considered the effect of the solar irradiation. By means of sunlamps, a value of 460 W m^{-2} was set during the fourth and sixth hours. The heat transfer coefficient, calculated according to the ATP agreement [30], could be increased up to 43%. The aerogel+RMF can reduce the heating effect due to the solar radiation by 27%.

Different from [79]'s concept, Zdun and Uhl [91] proposed the addition of a commercial SP-24 PCM layer, with thickness from 6 mm to 10 mm, to the inner face of an 8.6 cm Poly-Urethane foam insulation layer, as shown in Fig. 12.

The proposed innovative wall substituted one of the walls of a climatic room having 1 m³ of cold space inside. The experiments started at about -24 °C, being cooled down by a refrigeration unit, in order to
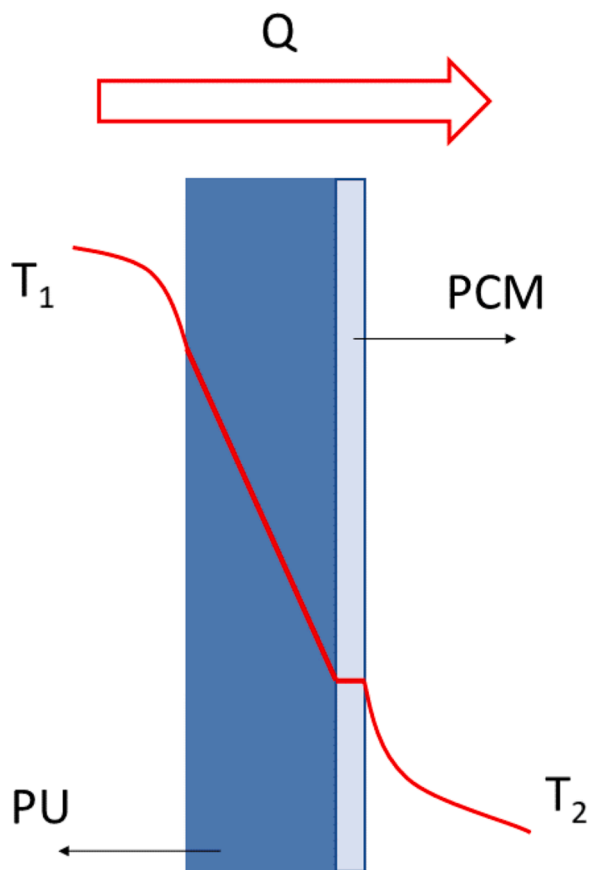
Fig. 12. Insulation wall proposed by [91].

ensure the PCM solidification (freezing temperature: -24 °C), to simulate the initial cooling stage of the refrigerated transport. This stage, which resulted in continuous on/off cycles of the refrigerated unit, lasted for

24 h and 40 h for the 6 mm and 10 mm layer, respectively. Once the target condition was reached, the refrigeration unit was completely turned off and only the ability of the PCM of acting as a passive cold source was monitored. The temperature evolution along time of the inner air was recorded to evaluate the overall performance. In particular, the time required to reach 15 °C in the cold space was selected as the monitoring variable for comparison purpose. By setting an external temperature of 22 °C, the 6 mm PCM layer reached the critical value about 6 h later than the reference case (no PCM), while it was around 30 h later for the 10 mm PCM layer. Therefore, the authors tried to verify the feasibility of the proposed solution as an alternative for a traditional semi-trailer diesel-driven refrigeration unit. A 13.2 m x 2.42 m x 2.45 m refrigerated cell was modelled. A 6 mm PCM layer was added to the cell wall. The analysis was run by means of the COMSOL software. To follow the ATP procedure, as done by [79], an external temperature of 30 °C was set. The authors aimed at evaluating the ability of the PCM in maintaining the temperature level lower than -20 °C, to make this solution suitable for transportation of frozen products. The results revealed that the inner temperature didn't exceed the targeted limit for more than 20 h. Moreover, 6 mm PCM layer distributed on the refrigerated cell walls resulted in about 900 kg, which is a value comparable to a big semi-trailer refrigeration unit. The authors also declared a 86% reduction in energy consumption with the novel system cooled down by an external electrical refrigeration unit (COP 1.5) compared with a traditional diesel-driven one (COP 0.2). Nevertheless, Zdun and Uhl [91] considered only the stationary case, the external solar radiation contribution was neglected and no food cargo inside the refrigerated cell was taken into consideration.

Similar to [91], Calati et al. [17] modelled a 2D section of a traditional European refrigerated truck insulation wall which consisted of a 5 cm Poly-Urethane foam layer wrapping a PCM layer with thickness ranging from 0.5 to 2 mm, as depicted in Fig. 13.

Since the authors proposed the innovative solution as an alternative for fresh foodstuff carriage, three different paraffin-based PCMs (RT2HC, RT4, RT5HC) with positive melting temperature (2, 4, 5 °C, respectively) were chosen. Moreover, to consider the effect of solar radiation on the heat transferred into the refrigerated space, the
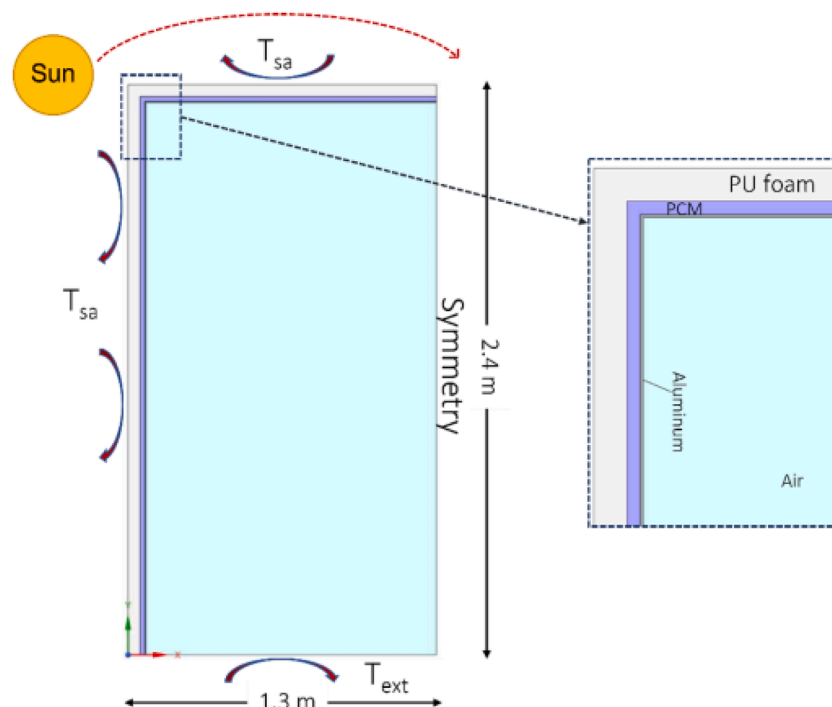

Fig. 13. 2D section of a traditional refrigerated truck [17].

temperature sol-air model was adopted (for details, the reader may refer to [130]). A temperature profile, standing for a typical summer day temperature trend for the city of Vicenza (Italy), was adopted as the base to estimate the hourly sol-air temperatures. The truck was supposed to be in operation from the 6AM to 4PM, therefore a period of 10 h was simulated. The numerical analyses were run by adopting the CFD software Ansys Fluent 18.2. The analyses started with the PCM completely solid and the refrigerated cell temperature at 2 °C. The ability of the passive cooling system in maintaining the temperature at an adequate level (under 8 °C) during the operating time was monitored. It was observed that the smallest thickness (0.5 cm) could ensure the health conditions for the most part of the entire route (8 h) but, when the PCM was almost melted, the cell air temperature increased reaching detrimental value for perishable fresh foods. Besides, the effect of the latent heat combined with the melting temperature on the cooling performance was investigated. By considering the same PCM thickness (0.5 cm), the RT2HC kept the cell air temperature for 10 h at 9.5 °C, RT4 close to 14 °C and RT5HC to about 8.5 °C. In fact, RT5HC, despite having the highest melting temperature value (5 °C), kept the cold air at the 10th h under the lowest value as it has a latent heat 47% and 25% higher than those of RT4 and RT2HC, respectively. When considering 1 cm layer thickness, the air temperature never exceeded 8 °C for all the three paraffins, demonstrating the validity of the innovative solution. Moreover, it was reported that assuming a 6-m-long refrigerated truck, the passive PCM cooling system would require about 200 kg of PCM which is lighter than the conventional refrigerating system as stated by Liu et al. [27]. This system should be cooled down during the depot period by a stationary electrical refrigerated unit being more efficient than a traditional mobile one, resulting in even higher emissions savings.

A different PCM location was investigated by Copertaro et al. [83]. In [17] and [91] the PCM layer faced the refrigerated space, whilst in [83] it was applied to the external side of a traditional 20′ ISO refrigerated container. The authors aimed at analyzing the advantages in terms of energy need reduction due to the application of the new container envelope. To reach this goal, a numerical FEM (finite element method) model in COMSOL Multiphysics environment was developed. In particular, a 6.058 m x 2.438 m x 2.591 m container was modelled having an insulation wall which consisted of 0.001 m external steel sheet, 0.03 m PCM layer, 0.10 m Poly-Urethane foam and 0.001 m internal steel sheet, as shown in Fig. 14.

Nine different PCMs were analyzed (from 27.5 °C to 46.5 °C), whose detailed characteristics can be retrieved from Tables 1 and 5. Milan, Ancona and Palermo were selected as the reference cities from which retrieving the data of the extreme summer weather conditions in accordance with UNI 10349 [131] to be applied as boundary conditions to the model. Moreover, five different exposures were considered: north,

Fig. 14. Section of the new envelope having the PCM layer. "2″ is the PCM layer [83].

south, east, west, and horizontal. As done by Calati et al. [17], the solar radiation was also considered. Compared with a traditional container, the authors evaluated the heat load peak and daily energy rate reductions to ensure the temperature inside the refrigerated space to be maintained at 0 °C. The internal air temperature was set at 0 °C, consequently, suggesting the adoption of an active refrigeration unit if considering a real application. Under the applied summer conditions, the RT35HC resulted the best PCM to be employed. In fact, it experimented delay in heat load peak of about 2 or 3 h. Moreover, heat load peak reductions from 20% to 20.9% and total daily energy rate reduction between 4.6% to 4.7% were calculated. The RT35HC was able to delay the complete melting and able to solidify during the night when the external temperatures are lower. Therefore, the heat could be transmitted into the cold space during the night, when high refrigeration unit performance and reduced energy costs occurred. On the contrary, RT42, RT44HC, RT47, and C48 did not perform properly as their phase change temperatures were too high, causing only partial melting. PCMs with melting temperatures lower than 35 °C were not able to address the required energy demand during the critical periods since they were completely melted during the first hours of the day. Based on [83], Fioretti et al. [84] experimentally studied the heat transfer performance of an insulation layer equipped with RT35HC on its external face. In particular, two experimental campaigns were conducted: an indoor and an outdoor one. For the indoor analysis an insulation prototype was developed whose main constituents were a 3 cm PCM layer consisting of RT35HC encapsulated in 81 polyethylene capsules sheet, and 10 cm PU-foam insulation layer. This prototype served as a wall of a small refrigerated test box put inside a climate chamber. The difference between the climate room and box temperatures was maintained at 19 °C. Moreover, a solar simulator (1000 W m^{-2}) was inserted in the climate room. The results of the test revealed a 59% reduction in the total energy for the PCM prototype wall. The external surface temperature remained at 63 °C against 90 °C for the reference case, suggesting the absorption of the solar irradiation due to the phase change process. Moreover, the internal surface temperature always remained 1 or 2 °C lower than that of the reference case. The outdoor campaign aimed at testing the proposed insulation wall in conditions closer to a real container. Therefore, on the external sides of a cold room (2.2 m x 1.4 m x 1.4 m) 3 cm of PCM layers contained in polyethylene capsules were mounted. The cold room presented a refrigeration unit ensuring the inside temperature is maintained at 0 °C. The external conditions were mimicking those of Ancona during summer in 2014, presenting maximum solar irradiation value at around 800 W m^{-2} and temperature from 13 °C to 28 °C. Even in this large-scale application, as already reported in [83], the PCM layer absorbed significant amount of heat under harsh conditions (intensive solar irradiation and high ambient temperatures). The authors chose two characteristic days to evaluate the performance of the PCM-based new application: 30/Aug/2014 and 09/Sep/2014. By considering only the value of the thermal flux peak, 5.5% (10.38 W m^{-2} and 10.99 W m^{-2}) and 8.57% (10.56 W m^{-2} and 11.55 W m^{-2}) reductions between the reference and the PCM cold room were found for the first and second selected day, respectively. However, the PCM significantly prolonged the time to reach the peak temperature. Delays of 4.5 h and 3.5 h were found for the two days, respectively. In particular, the heat flux peak occurred at 9 PM, when the cooling required by the refrigerator is lower, due to more favorable external temperature conditions. The more efficient operating conditions lead to lower energy/fuel demand, which can be easily translated into lower gas emissions. Similar to [84], Chandran et al. [132] investigated the integration of a PCM layer into the insulation wall of a refrigerated semi-trailer rigid box truck (13.56 m x 2.60 m x 2.75 m). The insulation wall consisted of a 0.03 m PCM layer sandwiched between a 0.035 m thick Stainless Steel 304 layer and a 0.05 m thick expanded polyurethane layer. Moreover, the internal face of the insulation wall was covered with a 0.005 m thick mild steel foil. Nine different PCMs were considered by the authors with different melting temperatures, coming from several suppliers. In particular, RT31, A31,
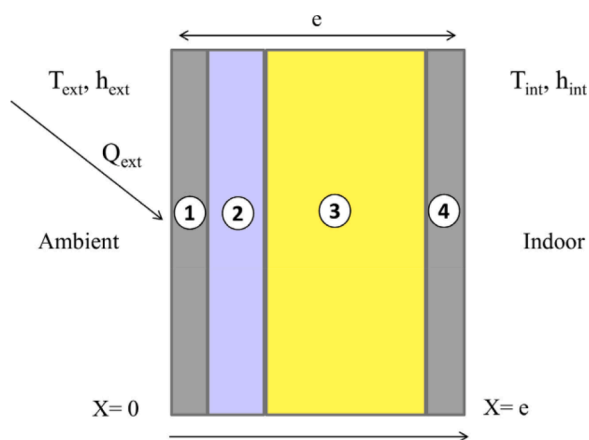
A30, PT29, A29, RT28HC, A28, PT28, PT 27, and A27 were tested. The authors analyzed the best solution in terms of energy savings, economic and environmental benefits. In details, they estimated the energy saving percentage, the payback period and the greenhouse gas emission (GHGE) reduction percentage. As done by [84], Chandran et al. [132] evaluated the refrigeration loads for each external truck surfaces exposed (or not) to the sun. The loads were calculated for two typical months in Kuala Lampur (Malaysia) by choosing a daily operation truck time period of 8 h from 7 AM to 3 PM. The authors assumed that the refrigerated semi-trailer was mounted on a mover for the transportation of frozen goods maintained at -10 °C. It was found that when 80 kg of A28 organic PCM was used, a maximum reduction of refrigeration load of 28.5% was reached. Moreover, 105 kg of PCM resulted in an additional energy saving with average load reductions of about 8.5%. From an economic point of view, the benefit-cost ratio exceeded unity for the top performing PCMs (A28, RT28HC, A29, PT28, PT29). The payback time of these top performing PCMs reduced as the masses increased, reaching a minimum of 2.07 years when 105 kg of PCM is employed. Like the payback time, the emissions savings increased as the PCM mass increased, with a maximum of 3060 kg CO_2/year saved by A28. Moreover, Chandran et al. [132] stated that if considering a longer travel distance, the advantages coming from the adoption of the PCM decreased and GHGE increased since a heavier vehicle consumes more fuel. However, compared with short-haul travel vehicles, a GHGE savings of 138 kgCO_2/year can be performed.

A different approach was followed by Tinti et al. [81], who aimed at developing an innovative insulating material having low thermal conductivity (good insulation properties) and, contemporary, good latent heat storage properties. Instead of adding macro-encapsulated PCM (in tubes, slab, etc.), as reviewed so far, hybrid poly-urethane foams with diverse weight fraction of micro-encapsulated n-tetradecane were developed. By measuring the surface temperature evolutions over time when subject to a radiative heater, the best composite material was selected and proposed for further utilization. To conduct the thermographic analysis, five different foams were prepared with different amount of PCM (0 wt%, 4.5 wt%, 7.5wt%, 12 wt%, 13.5 wt%). By means of a halogen lamp (1000 W) which simulated the external radiation and under room temperature set at 15 °C, the specimens were heated, and the surface temperatures were mapped.

Fig. 15 demonstrates the advantages associated with the integration of micro-encapsulated PCM inside the insulation foam material. As the PCM content grows, the temperature increase rate is lowered mainly because the heat us absorbed by the PCM and spent on phase change. Moreover, implementing the thermographic analysis, the maximum temperature difference between the reference foam and the composite one was detected. A maximum temperature difference of 3 K was observed for the lowest PCM content, 7 K for 13.5 wt% PCM. These
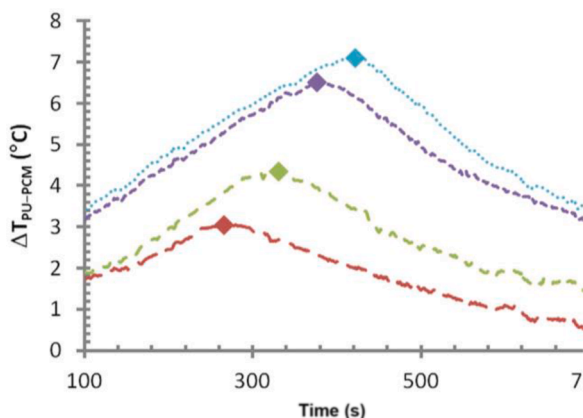
results suggest that the proposed hybrid foam, if translated into a hybrid insulation panel of a refrigerated vehicle for the transportation of perishable foodstuffs, can have a positive effect on reducing the cool loss when doors are opened and when a sudden refrigeration unit black-out happens or when significant solar irradiation changes along the route.

A hybrid insulation wall containing composite layer of poly-urethane foam and PCM (43 wt%, phase change temperature = 14 °C) for a refrigerated transport application was also investigated by Michel et al. [28]. The insulation wall, having a total thickness of 6 cm, consisted of two PU-foam layers sandwiching a composite PU-PCM one, as reported in Fig. 16. A reference case, only 6 cm of PU-foam, was also considered. To reproduce the operating refrigerated vehicle conditions, the authors imposed a temperature profile. A period of 8 h denoted as "cooling period", 8 h for "road delivery period" and 8 h for "door opening period". During the first stage, the upper face of the multi-layer, which represents the insulation side facing the external environment, was set at 10 °C. During the "road delivery period" the temperature was constantly increased up to 30 °C for 2 h, then maintained at 30 °C for 4 h, and then constantly decreased down to 10 °C for the other 2 h. Finally, during the last period, a temperature of 10 °C was set. The lower face, representing the interior insulation wall face, was maintained at 0 °C for the first two stages (16 h) and then set to 10 °C during the "door opening period". The authors numerically analyzed, in COMSOL environment, different scenarios by varying the thicknesses of the three layers making the insulation multi-layer. They verified that by inserting the PCM layer as closer as possible to the layer representing the vehicle exterior, the maximum reduction of the energy entering the cold space could be achieved (74.9 Wh m^{-2} against 78.2 Wh m^{-2}), since the cooling PCM capacity was exploited, correctly.

5.2. Refrigeration system equipped with PCM

In this section, the works regarding the adoption of the PCM as an integral part of the refrigeration system of a refrigerated vehicle are reported.

A novel refrigeration system concept for refrigerated trucks was proposed by Liu et al. [27]. As shown in Fig. 17, the system consists of an insulated Phase Change Thermal Storage Unit (PCTSU) in which the PCM is encapsulated inside flat containers. A new PCM was prepared, that is an inorganic salt aqueous solutions having melting and solidification points of -26.7 °C and -30.6 °C, respectively. The PCTSU is connected to an external electrical refrigeration unit which aims at freezing the PCM when the truck is stationary in the depot by means of a heat transfer fluid (Dynalene HC-40). On the contrary, during operation, the PCTSU is linked to a cooling unit which is located inside the refrigerated space. By adopting a thermostatically on/off controller the temperature
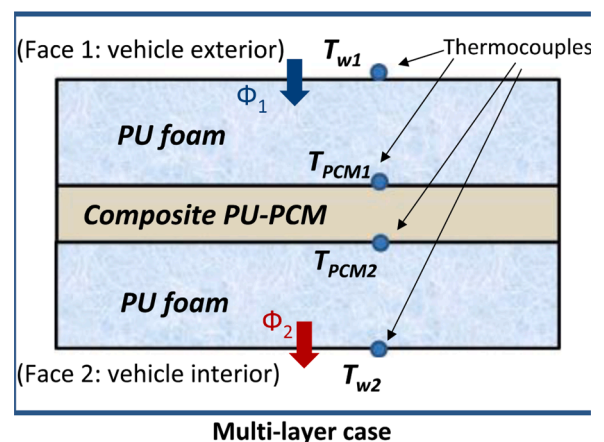

Fig. 15. Surface temperature over time trends of the different foam specimens [81].
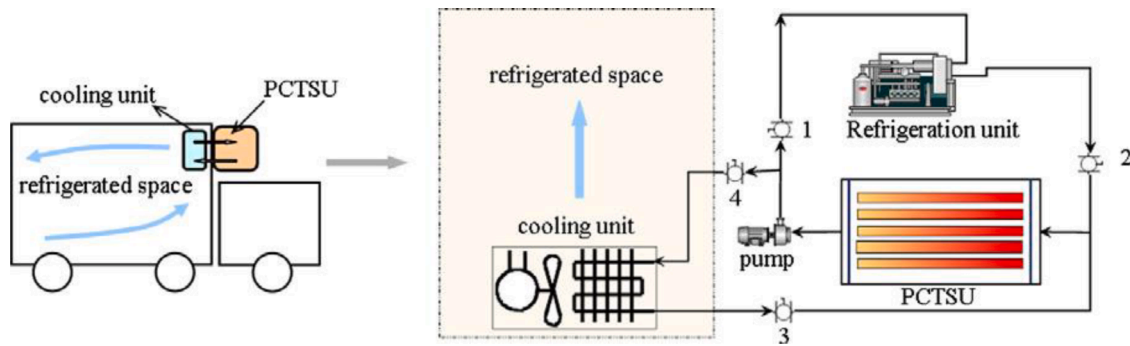

Fig. 16. Surface temperature over time trends of the different foam specimens [28].

Fig. 17. PCTSU developed by Liu et al. [27].

inside the refrigerated cell is maintained at -18 °C. The air is cooled down by the HTF circulating between the PCTSU and the cooling unit. The authors aimed at ensuring the appropriate target temperature for frozen food transportation for 10 h of a hot summer day in Adelaide (Australia). By means of the TRNSYS simulation program the authors considered the operating time from 8 AM to 6 PM. If a refrigerated space of 4.2 m x 2.4 m x 2.2 m is supposed, a total of 360 kg of PCM is required, by encapsulating it in 27 PCM container of 0.96 m x 0.52 m x 0.02 m, with a gap of 4 mm between two adjacent containers.

The potential of this system is the possibility of reducing energy cost and GHG emissions. Nonetheless, lower noise and maintenance required levels can be accomplished. Being the system employing an electrical stationary refrigeration unit, a more efficient and reliable cooling process is accomplished. The risks deriving from potential refrigeration leakages are also reduced. By using TRNSYS an annual refrigeration load of 4380 kWh was estimated. In this value, among several assumptions, 10 door openings/day and an average annual temperature of 17 °C were supposed. By considering different factors, such as the cost of diesel and energy (off- or on-peak) and the efficiency of the system (COP 1 or 1.5) or diesel engine (0.2) the authors estimated up to 86.4% cost reduction (off-peak fee and COP=1.5). More specifically, when a COP=1 and on-peak electrical fees are considered, 51% of cost savings can be reached. If COP=1.5, the reduction can increase to 67.3%. Finally, when an off-peak fee and lower COP (1) are taken into consideration, almost 80% reduction in cost can be materialized compared with a traditional diesel-based refrigeration unit. Besides, the authors reported that a cooling system for a refrigerated truck usually weighs around 370 kg, comparable with that of the proposed PCM-based system.

The potential of the innovative system developed in [27] was demonstrated and further developed in [80]. By assuming a typical refrigerated van, the daily cooling loads were estimated using TRNSYS. In particular, the transmission loads through roof, floor and walls, the heat load due to cooling unit equipment (fan motor, pump motor, etc.), the product load and the infiltration of the air during the door-opening periods were taken into consideration. A fully charging period of 8 h during the off-peak electricity fee period, that is from 11 PM to 7 AM, was supposed. Based on the climate data for the city of Adelaide (Australia), the maximum and the minimum loads were calculated. When considering the maximum heat load without door openings, it was obtained that from 8 AM to 9 AM of 14th of February, the cooling unit was able to cool down the refrigerated space from 25 to -18 °C by keeping the maximum pump speed. Just by regulating the pump speed, the temperature is maintained at -18 °C for an additional 10 h, ensuring the suitable conditions for frozen foodstuffs carriage. When the entire PCM in the PCTSU released its latent heat, the refrigerated cell temperature started to grow. If 20 door openings lasting 36 s each with an interval of 30 min between two subsequent openings were assumed, the cooling system would require an amount of PCM equal to 390 kg to ensure the desired safe conditions. In this situation, it was found that the temperature increased up to 8 °C during the door-opening period and,

the additional cooling energy requested to the PCTSU was accomplished by increasing the pump speed to recover the appropriate conditions. By tuning the PCTSU size, and the PCM amount consequently, the innovative system can be adapted for refrigerated van, trailer, or truck. For this letter, the PCM mass can be as high as 1000 kg if 20 door openings are considered. Since the refrigeration unit doesn't work when the refrigerated vehicle is in operation, the developed system can be assumed as a passive solution. In fact, the cold source is represented by the PCM and the only pieces of equipment consuming energy are the fan and pump motors; contributing only to a small fraction of the entire energy consumption of a refrigeration system.

An air heat exchanger containing the PCM, located inside the refrigerated space, and coupled with a traditional refrigeration system was, instead, developed and proposed by Principi et al. [85]. In particular, an air heat exchanger, consisted of six PCM flat aluminum containers encased in a polystyrene channel, was located close to the evaporator, as shown in Fig. 18.

Each PCM container has dimensions of 1.00 m x 0.03 m x 0.14 m. Moreover, since the temperature target inside the refrigerated space was set to the carriage of fresh products, the paraffin RT5HC with melting temperature of 5 °C, close to desired operating conditions (refrigeration unit is in operation to ensure the inside temperature level between 0 °C to 8 °C), was selected. A total of 19.15 kg of PCM was contained inside the air heat exchanger. A cold room (2.2 m x 1.4 m x 1.4 m), having 10 cm of polyurethane foam insulation layers equipped with a 1140 W cooling capacity unit was assumed as the refrigerated space of a refrigerated transport application. To investigate extreme conditions, the cold room was located inside a climate room maintained at 32 °C. The aim of the system was to enhance the energy performance of the refrigerated transport application by reducing the temperature fluctuations inside the refrigerated space under high external ambient temperatures. When the compressor was activated, the cold air exiting the evaporator passed through the air heat exchanger freezing the PCM. In fact, the average air temperature inside the refrigerated space was calculated to be 5 °C when the PCM was employed scenario and 3.68 °C for the reference case. During the OFF-time, the heat gain from the environment was absorbed by the PCM, lowering the temperature increase. Moreover, the ON-time of the compressor was prolonged with
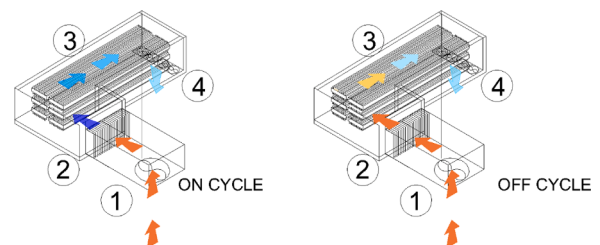

Fig. 18. PCM based air heat exchanger (3) close to the evaporator of the refrigeration system (2) [85].

PCM, but its ON/OFF-cycles were reduced. The authors stated that, by considering a reference period of 2 h, thirteen ON/OFF compressor cycles were needed for the traditional configuration, against six for the PCM system. The refrigeration unit efficiency increase led to a 16% reduction of the total electric power consumption, suggesting consequent reduction in GHG emissions.

The concept of installing PCM just after the evaporator of the cooling system of a small truck was also taken on by Ben Taher et al. [88], as shown in Fig. 19.

The authors numerically investigated the cooling performance of ten aluminum rods (2 m x 0.03 m x 0.1 m) encapsulating PCM, mounted on the ceiling of a small truck (1.6 m x 1.7 m x 3 m). The truck presented 10 cm of polyurethane foam insulation on the floor and 7 cm thick insulation layer on the other walls, being designed for the carriage of fresh perishable products (maximum temperature admitted: 12 °C). Moreover, the authors analyzed the effect of 15 min door openings after 60 min of refrigeration unit operation and compared the performances with or without the PCM. Firstly, the adoption of paraffin wax RT8HC was suggested. It was found that the PCM significantly lowered the temperature fluctuations inside the refrigerated space. In fact, as already demonstrated in [85], the cold air exiting from the evaporator is heated due to the effect of freezing the PCM before being released in the cold space. This let the cold space to be cooled down from 20 °C to 1 °C, and from 20 °C to 2 °C for the reference and PCM scenarios, respectively. Besides, when considering the door openings period, the mean cold temperature increased from 1 °C to 17 °C for the reference truck, and from 2 °C to 11 °C for the truck equipped with PCM rods, with consequent beneficial effects for the carried foodstuffs. The authors also simulated a long route scenario, that is with multiple close/open doors cycles (10 cycles) and, the performances of other two paraffins were investigated (RT3HC and RT5). It was revealed that RT5 is more suitable for middle distance route in which products like industrial milk, butter, and meats are transported. RT5, in fact, after the fourth close/open door cycles stabilized the temperature inside the refrigerated cell at 6 °C. The best performance was, instead, achieved through the employment of RT3HC. With RT3HC, the air temperature was maintained at 4 °C for a longer time, suggesting this PCM for the transportation of highly perishable foodstuffs. In terms of required cooling energy reduction, savings of 35%, 57%, 61% can be addressed when RT8HC, RT5, RT3HC are employed, respectively.

The ability of the PCM of ensuring suitable storage and transport temperature was also investigated by Orò et al. [78]. The authors wanted to analyze the thermal behavior of a "non-refrigerated" chamber, that is a space where the cooling is provided only by the phase change material. In particular, focusing on the refrigerated transport sector, the authors referred to non-refrigerated vans whose main aim is maintaining the temperature of frozen cargos only by the action of the insulation layer. A vertical freezer (370 L), with a 5 cm polyurethane insulation, was selected to replicate a small-scale van or other perishable products transportation units. Two different PCMs were studied to choose the one that ensured the best performance: Climsel C-18 (melting temperature -18 °C) and Cristopia E-21 (melting temperature -21.3 °C).
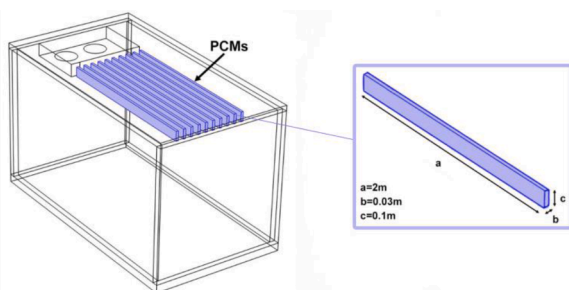
The PCM was encapsulated in seven stainless steel containers ($1.3 \cdot 10^{-3}$ m^3 each) and located on the food trays evaporator. Moreover, to investigate a real transportation scenario, product load was considered during the experiments, by inserting a total of 42 kg of M-packs. The freezer was placed into a climate chamber maintained at 25 °C to approximate the average European summer temperature. To evaluate the cooling performance of the PCM, the freezer was cooled down to -22 °C and then the electrical power was switched off. Significant improvements in lowering the temperature in the cold space to increase were calculated. The time to reach 0 °C was used as parameter to compare the different performances. It was obtained that in the reference scenario (without PCM) the system took 1.5 h to reach 0 °C, whilst 6.5 h and 8 h when C-18 and E-21 were employed, respectively. The reference cold chamber needed 11.5 h, against the one equipped with PCM which took 15.6 h and 21 h for C-18 and E-21, respectively. Moreover, against the two different PCMs, E-21 ensured that the air temperature could be maintained at colder values (between -16 °C and -12 °C) than C-18. The results suggest that the employment of PCMs for cold transportation can effectively enhance the transportation health conditions for perishable food carriages, by contemporary mitigating the polluting emissions.

A real scale refrigerated transport application was developed and experimentally analyzed by Tong et al. [89]. In particular, the passive cooling performance of an integrated rail-road cold chain container equipped with PCM was investigated. As shown in Fig. 20, the container is linked to an external charging facility, which consists of an electrical refrigeration unit, a heat transfer fluid (25 wt% Ethylene glycol acqueos solution) storage tank and a pump. A charging loop connects the PCM contained in ten cold TES plates (126 kg each) and the charging facility, to freeze the PCM.

The cold TES plate (1.8 m x 1 m x 0.1 m) consists of aluminum shell and embedded finned tubes. The container (12.92 m x 2.43 m x 2.896 m) is insulated by 0.1 m of polyurethane foam insulation material. Inside the container, nine TES plates are distributed on the ceiling, and one plate is mounted on the face opposite to the opening doors. Aiming at transporting fresh perishable products, the paraffin wax RT5 was selected as the best candidate, having a melting point of 4.96 °C and latent heat of 180 kJ kg^{-1}. To evaluate the system performance as a whole, different performance indicators were proposed, such as: charging rate, charging efficiency, system COP, energy consumption, cost reduction, emission reduction, and food quality indexes [89]. It was found that with a HTF previously cooled down to -5.5 °C, the charging system needed 6 h to freeze the PCM. As it can be deduced, the charging rate was faster during the initial stages when a great temperature difference between PCM and HTF occurred, then becoming slower. By considering the cold energy stored in the cold plates (PCM and aluminum encapsulation), moist air inside the refrigerated space and the HTF left in the cooling loop, an efficiency of 38.6% was calculated. The authors attributed this value to the long charging time which caused cold energy losses. However, if considering the system COP for the passive discharging process a value of 1.84 was estimated. This value, higher than the COP of traditional diesel-based refrigeration systems (COP ranging between 0.5 and 1.5), could be due to the constant operation of the large-scale chiller (without on/off cycles which normally occur during the cooling process in a refrigerated vehicle). Additionally, the proposed refrigerator was connected to the grid electricity, which improved the energy efficiency. The passive cooled container could maintain the temperature at an appropriate value (between 4 °C and 12 °C) for the entire 94.6 h route, despite facing very different external conditions (temperatures ranging between 13 and 35 °C). Compared to a diesel-powered refrigerated container, 86.7% reduction in the energy consumption can be achieved. This translates into an emissions reduction up to 78.5%. Four different food cargos, with different quality indexes, were considered: leaf lettuces, lettuces, strawberries, and mangoes. It was reported that the food quality was ensured. A complete analysis regarding the time evolution of relative
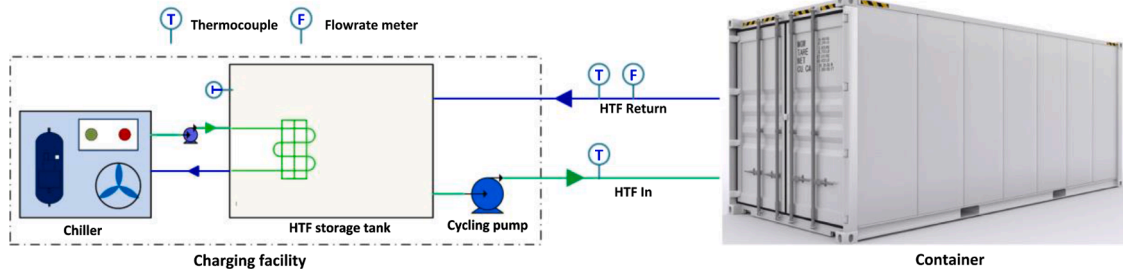

Fig. 19. Small truck equipped with PCM rods [88].

Fig. 20. PCM-equipped container linked to the charging facility [89].

humidity (RH) was assessed [89]. It was found that the innovative passive solution kept RH always between 80% and 90%, which is an optimal range for the transportation of fruit and vegetable crops. Moreover, the traditional cooling systems generally lead to lower RH values compared to PCM solution. The reason for the optimal RH performance was due to the fact that the passive system reduces the latent air heat transfer.

Liu et al. [103] developed a Phase Change Cold Storage Unit (PCCSU) and installed it inside the insulated compartment of a refrigerated vehicle, as depicted in Fig. 21. The PCCSU cools down the refrigerated space at different refrigerated temperatures, by setting different temperature configurations depending on the carried foodstuff. The novel unit is cooled down when the truck is stationary by exploiting the off-peak period, in order to make the cooling process more efficient and cost-effective.

The PCCSU consists of 24 stainless steel PCM plates, having a thickness of 3 cm and they are cooled down by the on-vehicle refrigeration system. When the truck is in operation, the cooling process relies on fans which below the air through the PCCSU being cooled down before entering the cold space. To be as close as possible to the temperature needed for the transportation of frozen products, three different target values of -14 °C, -16 °C, -18 °C were selected. Additionally, a PCM having a melting temperature of -30 °C with a latent heat of 175.3 kJ kg^{-1} was chosen. To assess the feasibility of the idea, the authors installed the proposed PCCSU inside an insulated container (5.00 m x 2.04 m x 2.00 m, internal dimensions) consisting of a 0.12 m thick polyurethane insulation layer and tested it experimentally. The mass of PCM was equal to 275 kg. Varying external temperature conditions were faced during the experiments, resulting, however, in an average external temperature of 29 °C. The set up could maintain the suitable conditions inside the refrigerated space for 16.6 h, 14.7 h, 10 h, presenting an average internal temperature of -12.3 °C, -14.5 °C, - 16.5 °C, when the target temperature of -14 °C, -16 °C, -18 °C were selected, respectively. Moreover, an economic analysis was conducted to verify the financial sustainability of the investment. Assuming that the truck was in operation between 8 AM to 6 PM, for 365 days per year and by considering 10 door-openings per day, the energy cost of the new PCCSU was compared with the traditional diesel engine-driven refrigeration units. It was reported that by adopting different COP values (0.5 – 1 – 1.5) and off-peak, basic, or on-peak energy fees, an energy cost reduction from 15% to 91% could be obtained, making the proposed solution
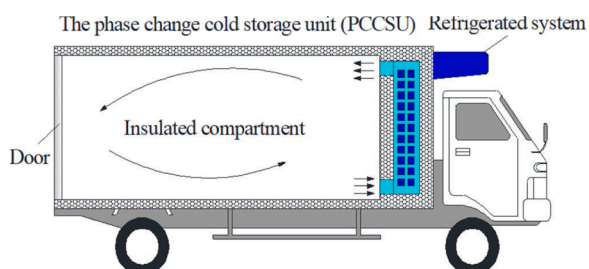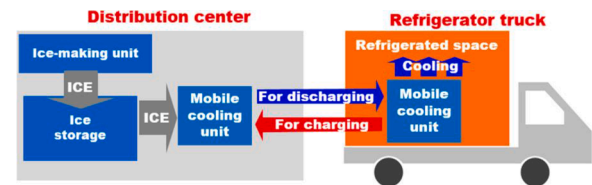

Fig. 22. Mobile cooling system [90].

as a promising one.

Ahn et al. [90] proposed an innovative cooling system for refrigerated trucks, consisting of an ice-making unit (IMU) used for the charging phase and a mobile air-cooling unit (MCU) during the discharging phase. In this concept, the phase change material role is played by the ice. In Fig. 22 the schematic of the mobile cooling system can be appreciated. The novelty of the proposed solution lies in the direct contact discharging process: in fact, the PCM is not encapsulated, and a direct cooling mechanism between the air to be cooled down and the ice occurs.

As shown in Fig. 22, the refrigeration unit, which is located in the distribution center, stores the cooling energy during the day, by generating ice cubes of different sizes. The MCU from the truck moves into the distribution center to be refilled with new ice cubes and then returned to the cooling cell of a refrigerated truck. A small-scale lab test apparatus was built to analyze the performance of the cooling system by varying the mass of the ice cube, the face air velocity, the amount of stored ice, the mass of an ice cube, and the inlet temperature. The COP for the IMU and a global COP which considers the entire cooling process (discharging and charging) were used to evaluate the integrated system performance. By considering only the ice-making unit, the COP of a 6.8 g ice cube was 28.5% higher than that for 10 g ice cube. The main role is played by the face air velocity and the amount of ice, with the highest COPs pertinent to 1.28 m s^{-1} and 6 kg. However, the COP was affected by the variation in the ice cube mass. The system average cooling capacities at 30 °C were 472.4% higher than those at 10 °C. Moreover, by evaluating a modified COP which considers the integrated system IMU and MCU, it was found that the ice mass cube strongly affected the power consumption of IMU and the fan power consumption of MCU.

The last concept to be presented here is the one proposed by Tan et al. [77]. The authors investigated the possibility of coupling PCM (water) and the cold energy recovery coming from Liquefied Natural Gas (LNG) refrigerated vehicles. In particular, a cold storage unit (CSU) was located and mounted at the ceiling of the refrigerated space. The CSU was insulated by 50 mm thick polyurethane foam and presented a cavity of 1.00 m x 0.15 m x 0.20 m hosting the PCM. A 1-m-long copper tube having an outer diameter of 20 mm and a thickness of 1 mm was immersed inside the CSU acting as a cold storage to freeze the PCM. Internally, the tube was cooled down by the cryogenic nitrogen gas which absorbs the heat from the (solidifying) water outside the tube. To improve the heat transfer performance, wave-like fins were added internally the tubes. The schematic of the proposed system can be appreciated in Fig. 23.
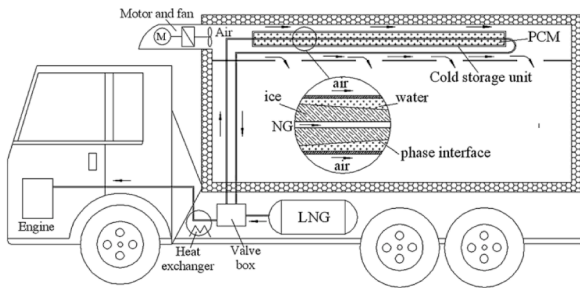

Fig. 21. The Phase Change Cold Storage Unit proposed by [103].

Fig. 23. LNG refrigerated vehicle coupled with the cold storage unit [77].

By means of a valve box, the LNG fuel circulates into the CSU and then evaporates. The superheated gas returns to the heat exchanger before being directed to the engine for combustion. To cool down the refrigeration space, the air is blown by a fan outside the CSU before being admitted to the refrigerated space. A comparison between this new concept and the standard one was not presented, nevertheless, significant emission reduction can be anticipated.

5.3. Eutectic plates

Eutectic plates can be considered as the most mature alternative to the conventional refrigerated unit installed in refrigerated vehicles as they have already found application in the market. It usually involves the use of eutectic mixtures made of sodium chloride and nitrate water solution [82] having very low melting points. The eutectic plates technology is also reported and regulated by the ATP agreement [30]. Therefore, in this section, only a few recent works, covering the use of eutectic plates into refrigerated container [82], refrigerated truck [87], medium refrigerated transport [133], and refrigerated truck trailer [134] are reported aiming at showing the application of this technology in refrigerated vehicles of different sizes.

Sepe et al. [82] applied FEM to study an innovative 20 feet refrigerated container equipped with PCM contained in eutectic plates for the carriage of fresh (between 1 °C and 4 °C) and frozen (from -20 °C to -18 °C) products. Moreover, the authors designed a passive equipment connected to a remote-control system and shaped air channels to ensure the cool air circulation and the stabilization of the internal temperature at the desired level. Different PCMs were evaluated to fill the eutectic plates and E-26 was finally selected due to its high latent heat value (260 kJ kg^{-1}) and relative low cost. Six eutectic plates were mounted on the ceiling of the refrigerated compartment. By means of fans, having 0.2 m diameter, 0.10 m^3 s^{-1} of air pushed through the cold plates and then is released into the cold space. Moreover, the air flow can be regulated to ensure a certain thermal gradient. All the information regarding container position and conservation status of cargo were monitored and registered by an electronic control system during the route. The container was insulated by a composite insulation wall consisting of polyethylene terephthalate (PET) foam sandwiched between thermoplastic matrix and glass fibers. The PET foam was selected aiming at limiting algae or bacteria growth, ensuring contemporary high structural property. It was found that this innovative PCM-based container can maintain the temperature inside the cool space at the desired level for almost a week. Moreover, the employment of fans and air duct ensured a good circulation of cold air, maintaining the relative humidity at suitable values. Besides, the new panel wall resulted in light and environmentally friendly design composed of recyclable material.

The installation of eutectic plates into a 6-ton refrigerated truck was instead proposed by Mousazade et al. [87]. In particular, the refrigerated box had dimensions of 2.05 m x 2.2 m x 4.8 m and was equipped with 6 cold plates and insulated by sandwich panels whose core consisted of 10 cm traditional polyurethane foam. Each cold plate was made of a parallelepiped macrocapsule (1590 mm x 690 mm x 52) hosting the

PCM and the 18 m long coil pipe. During the refrigeration period, that is the time needed to freeze the PCM, an expansion valve lets the refrigerant of the cooling unit (5.5 kW nominal power and COP = 3.5) to pass through the coil pipe inside the cold plate. The condensing unit was not incorporated on board, therefore, after the refrigeration period, the refrigeration system was detached from the vehicle and only the cold plates ensured the cooling enroute. The performance of three different eutectic solutions (E-26, E-29, E-32) was tested at four diverse truck speeds (80 km h^{-1}, 90 km h^{-1}, 100 km h^{-1}, 110 km h^{-1}) and the overall heat transfer coefficients were calculated.

As per Fig. 24, an increasing trend in the overall heat transfer coefficient versus the truck speed was reportted. This phenomenon can be attributed to the external convection that promotes heat transfer. The minimum heat transfer coefficient was obtained for E-26 at about 80 km h^{-1}. By monitoring the air temperature in the refrigerated compartment, the authors found a plateau at the melting temperature followed by a temperature rise increase after the melting was completed. Since among the different investigated PCMs, E-26 presented the lowest U values for all the diverse truck speeds, it ensured the longest keeping of appropriate transport conditions of frozen foods. It had, in fact, the longest melting time for all the investigated scenarios compared with the other eutectic solutions, due the lowest gradient between external and internal temperatures. Nevertheless, by considering concurrently the melting time at different truck speeds and the truck speeds themselves, the travelling distance (that is, the distance in which the suitable temperature is maintained) can be calculated. It was found that the longest travelling distance (almost 500 kg) was accomplished by E-26 at 110 km h^{-1}, since the higher vehicle velocity compensated the lower melting time.

A eutectic plates-equipped medium refrigerated vehicle was numerically analyzed by Radebe et al. [133]. In particular, the eutectic plates position was investigated aiming at finding the best configuration for the carriage of agricultural products. The best configuration contained two eutectic plates located on the ceiling of the truck insulated compartment keeping the temperature at 0 °C for five hours. For agricultural goods, entering at 15 °C, a refrigerated space temperature of 0 °C can be considered a suitable temperature level for transportation.

Numerical analyses aiming at investigating the heat transfer and fluid flow behavior of air of a refrigerated truck trailer equipped with eutectic plates were performed by Jeong et al. [134]. The authors focused on the door opening period. Different cold plate configurations were evaluated by setting the cold plates in a series mode opposite to the door openings or in series at the ceiling of the refrigerated compartment, as shown in Fig. 25.

The numerical analyses were conducted by running 2D simulations in CFX Ansys v19 environment. An external air temperature of 293 K was fixed. Moreover, the effect of the presence of the cargo, and the suction or blowing configurations of the fan were also investigated. Five boxes full of frozen meat were added in the truck trailer. The cold plates' temperature was set at -29 °C, as the typical melting temperature of a eutectic mixture. When the compartment was empty of foodstuffs, it was
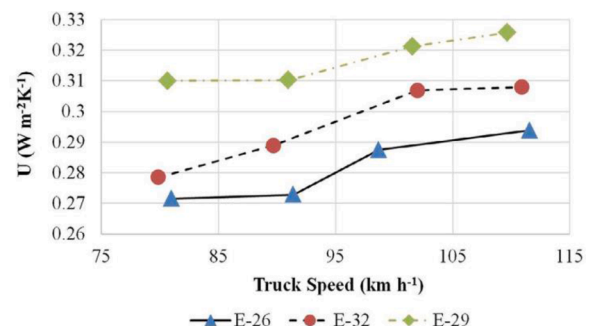

Fig. 24. Overall heat transfer coefficient varying with the truck speed [87].
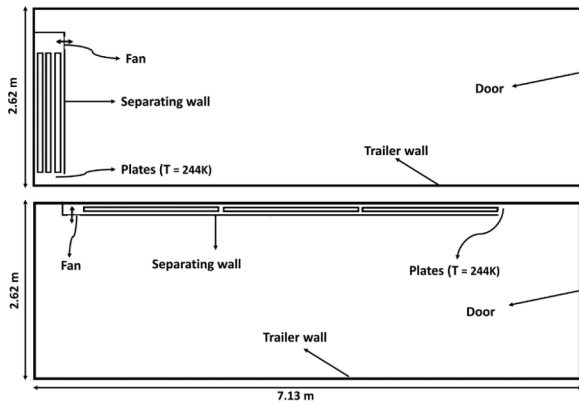
Fig. 25. Different cold plates positions [134].

found that the best configuration dealt with the cold plates set in series at the ceiling. In this configuration, recirculation zones could be detected which prevented the hot air to infiltrate from the outside environment. This recirculation zones were cut off when the cargo was added. Moreover, when the eutectic plates were at the ceiling level, the presence of the cargo caused blockage of air and therefore a pre-existing flow inside the trailer was found. The consequent effect was the possibility of the external hot air to find preferrable paths to enter quicker inside the cold compartment. As a result, the higher maximum temperature for the foodstuff was observed. Nevertheless, by considering that during the route the amount of cargo boxes progressively decreases, the authors stated that the configuration showing the cold plates mounted at the ceiling can improve the performance since, as the number of cargo boxes decreases, it tends to reach the empty cargo scenario.

6. Phase change materials in cold storage boxes for distribution of perishable products

As stated in the introductive section, the distribution of the temperature sensitive products is a crucial activity which usually occurs during the last stages of the cold chain. Appropriate distribution conditions are fundamental to ensure the safety and the quality of the products to the final consumers. The perishable products delivery is normally accomplished by the employment of insulated box or specific packages which preserve the products themselves. As reported in the previous section, some passive system involving the adoption of phase change material for refrigerated transportation have been developed demonstrating promising results. The same concept may be applied for a cold storage box: the integration of PCM to improve the cooling capacity maintaining the suitable product temperature during the distribution.

A cold storage package was experimentally and theoretically investigated by Kozak et al. [92]. In particular, two different packages were tested. The smaller package consisted of a 4 mm thick fitting cardboard box (32 cm x 25 cm x 25 cm), a high-density polystyrene insulation layer which formed a cylindrical cavity in which a double wall plastic container was inserted. The plastic container hosted a green aqueous salt solution PCM (melting temperature of -10 °C) in the double wall cavity, leaving space for the products in the inner cavity. On the contrary, the larger box consisted of a 4 mm thick cubic cardboard box (side of 50 cm), a high-density polystyrene insulation layer with a cylindrical cavity to host 4 arched bottles filled by purple aqueous salt solution PCM (melting temperature of -33 °C) which wrapped a cylindrical plastic container of the delivered product. The water was selected as the product to be transported by means of the cold boxes. The PCM was cooled down to -70 °C in order to ensure its complete solidification, and the experiments lasted until product temperature was close to the ambient one.

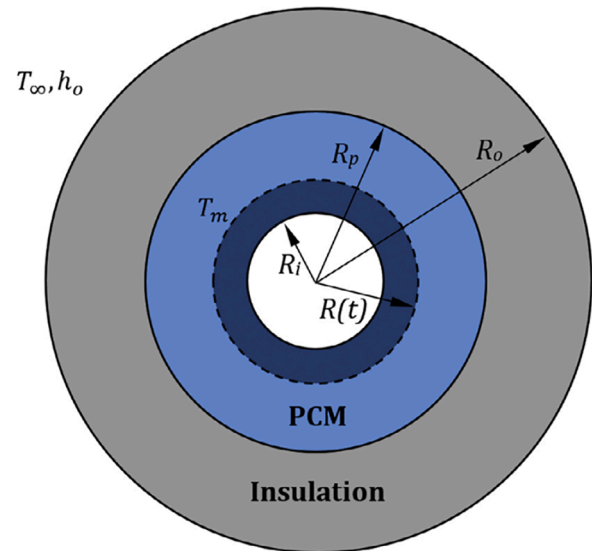Based on experiments, a one-dimensional analytical model was

Fig. 26. Analytical model [92].

developed. Moreover, one- and two-dimensional numerical models were developed in Ansys Fluent 13 environment. The theoretical analysis based on the analytical and numerical models aimed at finding the best configuration among the different parameters (as shown in Fig. 26) which prolonged the melting time finding the optimal insulation thickness. For additional details, the reader may refer to [92]. From the analysis, it was found that an optimal ratio between insulation thickness and PCM thickness existed which let to maximize the melting time. Moreover, the results revealed that the melting time is strictly affected by the ratio of the PCM thermal conductivity and insulation one. Almost negligeable dependance from Biot number was demonstrated. All of these results must be carefully taken into consideration when designing an optimal cold box. Besides, the 2D numerical model carefully predicted the experimental results, and the authors stated it can be a useful instrument to support the design stage by investigating different materials, dimensions and operating conditions.

Huang and Piontek [93] developed a cold chain insulated box for the transportation of perishable products at a temperature level ranging from 2 °C to 8 °C. The authors improved the box performance by the insertion of PCM.

As shown in Fig. 27, the insulated box (540 mm x 420 mm x 480 mm) had insulation walls which consisted of a triple layer of 10 mm polyurethane foam, 10 mm vacuum insulation panel, and 10 mm polyurethane foam. Two different PCMs (water and OP5E, melting point 0 °C and 5 °C, respectively) were encapsulated into two different high-density polyethylene slabs having dimensions of 350 mm x 290 mm x 15 mm. Since the PCM equipped insulation box aimed at keeping the desired temperature (2 °C to 8 °C) under diverse external conditions, three scenarios were investigated: *extremely high temperature condition*, during which the water and OP5E started at 0 °C and 5 °C, respectively, with chamber temperature of 35 °C; *extremely low temperature condition*, during which only OP5E panels were adopted and the controlled climate room temperature was set at -20 °C; *alternating temperatures condition*, during which the external temperature was set at 35 °C for the first half and -20 °C for the last half. When adopting only water as PCM, it was found that under extremely high temperature condition, the air temperature inside the cold box can be maintained at the appropriate level for more than 78 h, whilst only 54 min whit the box empty of PCM. Moreover, the addition of OP5E layer assured the air in the cold space to be maintained under 8 °C for 81 h. Under extremely low temperature the box ensured the suitable transport temperature for only 62 min. The addition of the water slabs let the temperature to be lower than 2 °C after 10 h, whilst the combined effect of OP5E and water assured 102 h of
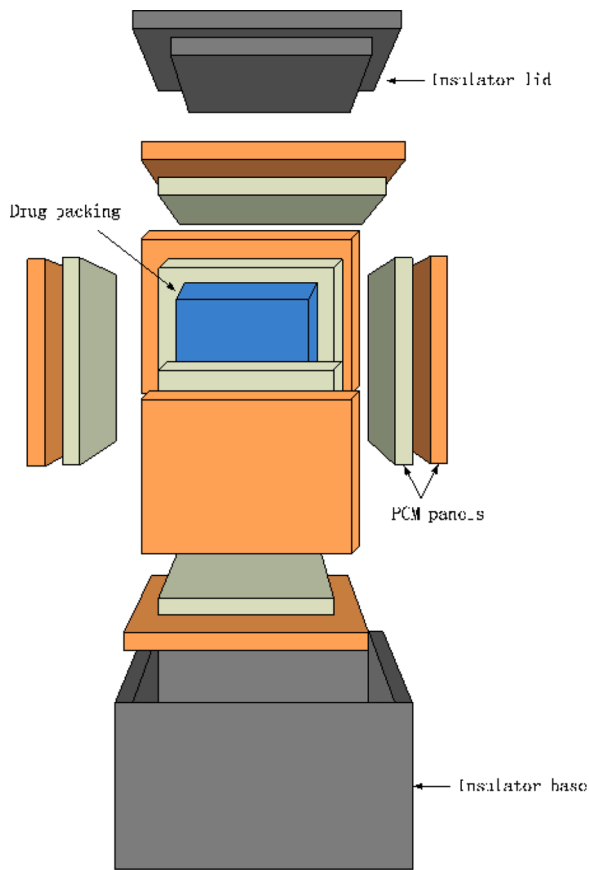
Fig. 27. PCM based cold chain insulated container [93].

appropriate air temperature level. Under alternating external temperatures, it was found that OP5E and water ensured the temperature between 2 °C and 8 °C for 100 h. In [93] it was shown that the right PCM selection is crucial to contribute to the extension of the shelf-life of perishable products during the transportation.

The importance of the appropriate PCM coupled with the optimal PCM arrangement for the cooling performance of a cold energy storage portable box was deeply analyzed by Du et al. [94]. The box had external sizes of 430 mm x 285 mm x 345 (length x width x height). Five different configurations were studied by varying the PCM location maintain the same PCM amount (1371.75 cm^3): case 1 presented the PCM entirely located at the box ceiling, case 2 20% of PCM on the four sides and 20% on the top, case 3 25% of PCM distributed on the four sides, case 4 20% of PCM on the four sides and 20% on the bottom, and, finally, case 5 having the PCM entirely located at the bottom of the box. Different performance indexes were proposed such as the cooling time, that is the time in which the central box temperature remains under than 8 °C (temperature limit for the transportation of fresh perishable products), the discharging efficiency, i. e. the amount of provided cooling energy

against how much of it could have been provided, and, the discharging depth, that lets to quantify the amount of cold energy remained in the cold plates.

By employing the wax paraffin RT5HC as PCM, it was found that, under an external temperature of 25 °C, the longest cooling time (9.5 h) could be reached by considering the PCM equally distributed on the top and sides of the cold box (case 2). Case two also showed the highest discharging depth value (74.1%). In fact, by observing Fig. 28, in the case 2 configuration, almost melted PCM can be found in the cold plates, suggesting the appropriate exploitation of the cooling energy which can be supplied by the phase change material. By fixing configuration 2, the effect of other wax paraffins were tested (RT0, RT2HC, RT3HC, RT4, RT8HC, with 0 °C, 2 °C, 3 °C, 4 °C, 8 °C melting points, respectively). It was found that the lower melting point led to a higher discharging depth and longer cooling time consequently. Moreover, a lower melting time ensured a higher thermal difference between external and internal temperature which caused higher heat transfer rate. Therefore, the best trade-off, was obtained by employing RT2HC. Finally, by modifying the insulation material, changing from traditional poly-urethane foam to vacuum insulation panel (VIP), a longer cooling time was reached (46.5 h against 9.6 h).

Similarly to Du et al. [94], Burgess et al. [104] aimed at optimizing a portable phase-change material storage system for cold chain delivery fresh foodstuffs applications. In particular, the authors evaluated three different layouts, by locating the PCM containers on the top and bottom of the box (layout 1), only along the sides (layout 2) or uniformly on top, bottom and sides (layout 3). To assess the best solution, the ability of the system to maintain the majority of the contents under 5 °C was chosen as an important performance indicator for the comparison. The authors firstly run experiments by adopting the "layout 1", i. e., by using PCM bricks (total amount 2 kg) on top and bottom of the box (internal dimensions: 500 x 300 x 180 mm^3). The cold space was filled with M-Packs and filler packs to replicate the fresh cargo. The temperatures at different locations were monitored over time and a numerical model in Ansys Fluent was developed and validated based on the experimental results. Therefore, the different layouts were investigated, and it was found that the uniformly distributed PCM let to reach the longest time under the temperature threshold of 5 °C (15.8 h). This value is significantly higher if compared with the reference case (without PCM) which ensured the suitable conditions for 5.3 h only. Nevertheless, "the layout 3" presented a significant temperature deviation (± 5.64 °C). The best performance in terms of temperature uniformity among the contents was obtained by adopting the "layout 2" configuration. This result shows that when designing the best cold storage box, the content typology must be considered: for example, for high-value perishable products (such as medicines, etc.) the local temperature uniformity inside the cold space (without hot spots possibly) is more important than the average value of the cold space temperature under a specific threshold. Moreover, the authors analyzed the effect of four different PCMs, water, potassium sorbate (PS), tetradecane + ducosane (TD) and tetradecane, having different melting points and latent heat values. It was found that the highest latent heat let to prolong the time the system was under the temperature threshold, while a lower PCM melting points permitted to
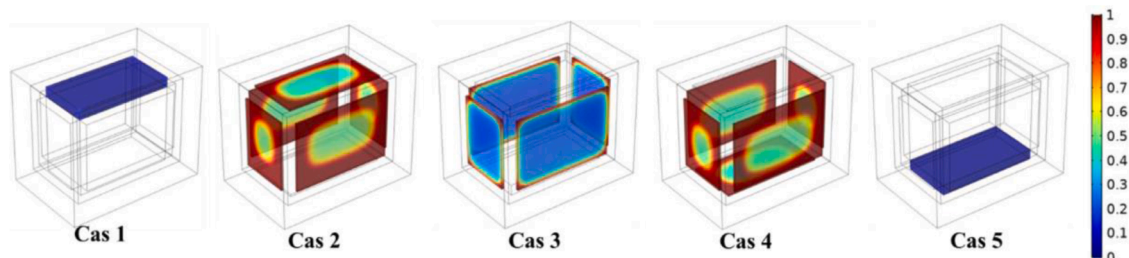

Fig. 28. Liquid fraction for the five different investigated cases in [94].

obtain a higher discharging efficiency but temperature inhomogeneity contemporary.

The thermal performance enhancement of a portable box equipped with phase change material (PCM) was also studied by Nie et al. [95]. A composite PCM was developed, consisting of RT5, fumed silica (SiO₂) and graphene. The cold box presented external dimensions of 460 mm x 300 mm x 340 mm (length, width, height, respectively) having 30 mm of poly-urethane foam insulation material on the walls. A total of 8 high-density polyethylene PCM containers (28 mm x 120 mm x 190 mm) were inserted inside the cold box: four at the top, and the rest in proximity of the internal walls. The amount of the adopted PCM was 2.64 kg. Bottles filled with water (2 L) were used as the transported temperature-sensitive product. The PCM were frozen by means of a freezer having -19 °C as set point temperature. To evaluate the cooling performance of the PCM, the box was set in a climate chamber maintained at the temperature of 30 °C. As done by Du et al. [94], the discharging phase ended when the transported goods reached the temperature of 8 °C. As Du et al. [94], the cooling duration index was adopted to evaluate the cooling performance. Moreover, the charging and overall energy efficiencies were calculated. The former was formulated as the ratio between the sum of the sensible and latent heats exchanged by the PCM and the energy requested to cool down the PCM itself. The overall efficiency, instead, was defined as the ratio between the energy absorbed by the products (water) and energy consumed to freeze the PCM. As stated in Section 3.4, the leakage occurrence is a great drawback when employing PCM, especially when dealing with food transportation. Therefore, by adding 4 wt% to the RT5 PCM, the authors found that the leakage issue might be overcome. Moreover, the composite PCM presented good cyclability, having thermophysical properties almost constant even after 200 cycles, with melting point close to 6.5 °C. By considering the cooling performance of the box, it was found that the pure PCM ensured 11.8 h of cooling time, whilst 11.35 h the developed composite material, since this latter had a slightly lower latent heat value (131.86 kJ kg⁻¹, against 143.74 kJ kg⁻¹). However, if focusing only on the charging time, the composite PCM presented a solidification time which was 11.5% shorter than the pure one, which increased the charging efficiency by 6.09%. Additionally, the composite PCM enhanced the overall energy efficiency by 12.58%.

With the aim of developing a phase change material with transition temperature between 2 °C and 8 °C to be employed in vaccine cold storage equipment, Zhao et al. [96] added expanded graphite (EG) into a mixed tetradecane (TD) and lauryl alcohol (LA) solution to obtain a new composite PCM. The insulation box had vacuum insulation panel as insulation material. The box possessed a shell with hollow plate structure, with the space inside the shell hosting the cold storage agent. The cold storage box (shown in Fig. 29) had dimensions of 200 mm x 95 mm x 55 mm. It presented a storage hole in which the vaccine reagent tube could be inserted.

It was found that a so developed vaccine box could exchange the cold energy in a more proper way, keeping the temperature of each vaccine tubes at a suitable level and reducing the temperature fluctuations during the transportation. To evaluate the cooling performance, no-load and load scenarios were investigated. During the first scenario, three cold storage boxes were inserted in the cold insulation box with 6 cold plates arranged around. A varying external ambient temperature from 28.2 °C to 40.6 °C was detected. It was obtained a cooling time (time in which the temperature inside the box was maintained between 2 °C and 8 °C) of 47.73 h for the vaccine box. The top plate inside had a cooling time of 40.78 h. For the load scenario, yoghurt was inserted inside the box, due to its intrinsic temperature sensitive nature, being viscous and acid. The temperature between 2 °C and 8 °C was maintained for 52.36 h if considering the cold storage vaccine box, whilst only 44.05 h for the top plate, with an average cooling time of 46.04 h. The so developed new cold chain equipment ensured the required vaccine transportation temperature for a long-time, preserving its quality.

PCM to be employed in vaccine cold boxes was also analyzed by Ray et al. [97]. They numerically investigated the cooling performance when a temperature interval from -55 °C to -40 °C is required. The SP-50 PCM was selected as the best solution to accomplish the temperature constraint. By means of CFD analyses, two different portable cold storage boxes were studied by maintaining the same constituting materials and amount of PCM. Cuboid and cylindrical configurations were modelled. The cubic box presented polyurethane insulated walls distributed on the inner sides, having 394 mm x 290 mm x 350 mm as external and 324 mm x 220 mm x 270 as internal dimensions, respectively. By assuming the same insulation material, the cylindrical container consisted of an outer diameter of 371.1 mm and internal one of 285.8 mm, with the gap filled by PCM. The numerical started with an internal temperature of -55 °C to ensure the PCM was completely solid, and the time in which the temperature was under -40 °C was monitored. Two different external summer conditions were considered and applied: a temperature of 45 °C or 30 °C. For both the scenario, the cylindrical configuration showed better cooling performance, due to low surface area to volume ratio of the cylinder. Under 30 °C, the cuboid box resulted in a cooling efficiency of 55.14% and cooling time of 15.4 h. On the contrary, the cylindrical box led to a cooling time of almost 19 h with a cooling efficiency of 60%. The authors reported that this type of passive regulation temperature can be adopted for the storage and transportation of highly temperature sensitive products, such as Covid-19 vaccines.

Liu et al. [105] developed a highly efficient cold box for smart cold chain logistics. They adopted an eutectic brine in Super Absorbent Polymer (SAP). The PCM brine consisted of potassium and ammonium chlorides dissolved in water. The homemade PCM had a melting point close to -21 °C with a latent heat of 230.62 kJ kg⁻¹. This novel PCM also presented relatively high thermal conductivity (0.589 W m⁻¹ K⁻¹), high-cost effectiveness (0.00000763 $ J⁻¹), negligeable supercooling and good cyclability. The PCM was located along the sides of the box and the cold storage times when transporting aquatic or biological samples were monitored. In the first scenario a cold storage time of 21.44 h was obtained whilst 16.37 h for the second case. Moreover, the authors provided temperature sensors and GPS position system in order to monitor the real-time thermal performance by an external device (as a smartphone, etc.)

A cold storage box for the transport of fruits, vegetables and other agricultural products was experimentally tested by Xu et al. [98]. Different PCMs were employed in order to verify which one ensured the desired conditions (temperature of cold space maintained between -5 °C
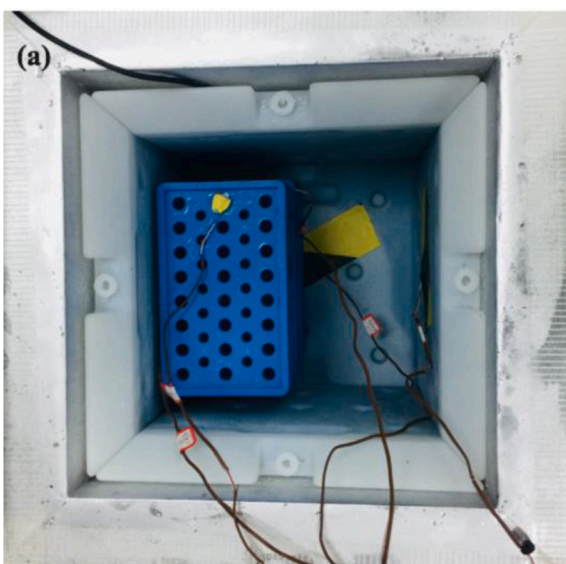

Fig. 29. Cold storage box inside cold insulation box [96].

to 8 °C). In particular, water (PCM1), water + 1 wt% sodium poly-acrylate (PCM2), and water + 1 wt% sodium polyacrylate + 0.1 wt% multiwalled carbon nanotubes (MWCNTs) (PCM3) were adopted. All the PCMs had phase change temperature of about 0 °C. The PCM was contained in 4 polyethylene cold plates, inserted around the internal walls of a vacuum insulation box having external and internal size of 320 mm x 275 mm x 280 mm and 200 mm x 200 mm x 200 mm, respectively. The experiments were run with an external temperature of 15 °C ± 3 °C. The cooling capacity of the cold plates was investigated, and the experiments were stopped when an average internal temperature of 10 °C was reached. The effect of the presence of transported products was also analyzed by the insertion of four caps of yoghurt in the available space between the composite layers made of VIP panel and cold plate. When only water was used, the yoghurt was maintained at the desired for about 56 h, with a cold space temperature of 6 °C. When employing PCM2, an extension of the constant temperature phase inside the cooling box was extended of about 9 h, with a temperature lower than 6 °C for 4.5 h more than what done by PCM1. Moreover, when using PCM3, the time in which the temperature was maintained under 6 °C was 87 h. The combined effect of good insulation material and PCM with good heat transfer properties (especially, enhanced thermal conductivity) can create suitable conditions for the transportation of temperature-sensitive products.

By means of numerical analyses, Xiaofeng and Xuelai [99] designed and studied a multi-temperature insulation box presenting two different phase change materials. PCM1, n-octanoic acid-myristic acid composite (7.1 °C phase change temperature, 146.1 kJ kg^{-1} latent heat), and PCM2, potassium sorbate-water composite (-2.5 °C melting temperature, 256.2 kJ kg^{-1} latent heat), were combined with vacuum insulation panels to create three zones at different targeted temperature inside the cold compartment. In particular, zone1 (Z1) was destined to dry products that do not require specific temperature to be transported, zone2 (Z2) with a range between 7 °C and 10 °C for the transportation of melon, pumpkin or some other fruit and vegetable, and a colder zone (Z3) for hosting more temperature-sensitive products, which require a cold space to be maintained between -3 °C and -1 °C. The insulation box consisted of 30 mm polyurethane and vacuum insulation bord sandwiched between two 2.5 mm thick iron plates. Moreover, since the authors wanted to design a box which could ensure the appropriate transport condition with an external environment temperature of 298 K, 13.8 kg of PCM1 and 12.1 kg of PCM2 were inserted in the multitemperature cold box. A roller was arranged, aiming at tuning the size of the different compartment based on the different transported loads need. When the box was experimentally tested, it was found that the temperature inside Z2 was maintained at 7 °C for 13 h. In the coldest zone, the desired temperature of -2 °C was ensured for 13 h, while the temperature for the carriage of dry products remained at 19 °C. More recently, Guo et al. [100] developed a novel cold storage box aiming at investigating the effects of three parameters, such as, the amount of PCM (eutectic salt, melting temperature: -80 °C), adjustment plate opening rate and storage plate heat transfer area on the temperature increasing rate and temperature distribution in the cold space. The box had dimensions of 1000 mm x 500 mm x 500 mm with insulation layers consisting of 2 mm of nested glass, 30 mm of poly-urethane and 20 mm of vacuum insulation board. The system was cooled down by liquid nitrogen injection. The statistical techniques of the variance analysis and response surface methodology were adopted to investigate the relation between the above-mentioned parameters. It was found that the temperature increase rate and the temperature standard deviation were affected by the coupling of the storage plate heat exchange area (varied from 0.09 to 0.11 m^2) and the amount of PCM (varied from 1.3 kg to 2.6 kg). Moreover, the adjustment plate opening rate was varied from 20% to 40%. It was obtained that the temperature standard deviation decreased as one of the parameters increased, while an increase in one of the parameters generated a temperature elevating rate increase.

The idea of adding PCM slabs to the walls of an insulated cold box,

was used by Orò et al. [101] to develop an active phase change material package for an ice cream container. The authors, in fact, aimed at enhancing the quality of the ice cream when maintained outside the freezer, by modifying its thermal protection. In particular, the dead zones of a common 5 L ice cream container were filled by PCM (E-21 with 2%wt of oxethylmethylcellulose as thickening agent to prevent PCM leakage), as shown in Fig. 30. Moreover, 2 cm of additional PCM layer was added to the bottom of the container.

In order to ensure the complete solidification of the ice cream and PCM before the beginning of the experiments, the container was maintained at -28 °C. Then it was located in a climatic chamber set at 25 °C. By monitoring the temperature evolution over time, it was found that the use of PCM let the ice cream to be subjected to less temperature differences along its volume. In particular, the central part of the ice-cream remained 3 °C lower if PCM was adopted (-15 °C, against -12 °C). Greater temperature gap was, instead, calculated at the corner (-15 °C for the PCM solution compared with -5 °C for the reference container). Smaller temperature zone differences in the ice cream are beneficial for the ice cream quality itself. By the development and appropriate validation of a numerical model, by modifying the PCM thickness, the authors investigated different scenarios. The obtained results were compared by using the period factor, that is the ratio between the time needed to reach a determined temperature when the PCM was or was not considered. High thermal protection was obtained by adding 20 mm of PCM at the container sides whilst 10 mm at the bottom. This new configuration ensured the optimal protection by occupying a volume which is only 7% larger than the reference container.

Leducq et al. [102] also analyzing the contribution of the PCM to the thermal protection enhancement of ice cream during storage and transportation. The authors conducted experiments by inserting three rectangular cardboard boxes, each of them containing eight 1 L ice containers (100 mm x 100 mm x 70 mm) in a freezer. To the cardboard, PCM (Cristopia E-21) rectangular bricks (220 mm x 150 mm x 25 mm) were added to the walls. Even the solution concerning the thermal insulation improvement by the addition of 25 mm thick expanded polystyrene to the cardboard box was investigated. The reference and the two modified cardboards were subjected to same storage conditions, that is 140 days at a mean temperature of -22 °C, to analyze the long-term storage. The crystal size (which reflects the product quality) was used as the parameter to compare the different thermal performances of the three cardboards. Significant smaller crystal sizes were identified for the cardboards with PCM. The PCM also let to enhance the thermal protection by using a smaller thickness compared with the polystyrene added box, assumed a similar damping effect. To analyze the thermal protection under thermal abuse condition, the boxes were exposed for 40 min at the ambient temperature (20 °C). Only 1 °C

Fig. 30. PCM-based ice-cream container [101].

temperature rise was detected when PCM was used, demonstrating its great contribution in increasing the maintaining of the safe condition during the transportation of perishable products.

7. Conclusions and future challenges

In this review, the works retrieved from the literature involving the adoption of PCM in applications along the cold chain were presented and discussed.

In particular, this review focused on the transport and distribution stages. Moreover, for a better understanding of the topics, two introductive sections were proposed to make the reader conscious of what PCMs are, their advantages and main limitations, and how currently is the cold chain transportation managed, highlighting its weak aspects (high energy consumption, greenhouse gas emissions, etc.)

From the surveyed works, it is clear that different solutions have been investigated, so far. Focusing on the refrigerated transportation, two important macro-categories were identified, the modification of the insulation layer by the insertion of the PCM, or the designing of a novel refrigeration system which exploits the PCM. Moreover, the studies involved the possibility of designing a complete (or almost complete) passive cooling system or an active one. When the PCM is added to the insulation walls, it was found that two different goals might be achieved: reducing the heat load peak and the heat transferred into the refrigerated space or acting as a cooling source. In the first scenario, a PCM having a melting temperature close to the outer temperature (usually ranging between 18 °C (summer night) and 35 °C (summer day)) has been reported to be the best solution, since, by exploiting the latent heat, the incoming heat is absorbed during the critical hours and released after a certain period, under more favorable conditions for the cooling unit (for example, during the evening, if a complete summer day is considered, when the external temperature is lower). It is clear that such idea requires an active system, even if energy consumption emissions reductions, compared with the traditional solutions, have been stated to be achievable. The great advantage is, therefore, the possibility to cool down the PCM of the developed LTES system during the night, without requiring the employment of an additional refrigeration unit.

On the contrary, if the direction goes to the design of an insulation wall incorporating PCM to act as cold source, it has been suggested to locate the PCM in the internal side of the insulated wall, that is facing the cold space. The temperature of the PCM is, in this case, close to the carriage targeted temperature. Therefore, it usually ranges between -20 °C to 5 °C, depending on the cargo typology (frozen or fresh products). The PCM on the wall acting as cold source may take to the development of a complete passive refrigerated vehicle. The PCM, being refrigerated when the vehicle is stationary in depot, releases the cold during the operation. This solution may conduct to remarkable savings in terms of reduction of energy consumed and polluting emissions. In fact, it lets to drop out the dependency from fossil fuel-based refrigeration system, since the latent thermal energy storage system may be charged by an electrical and more efficient stationary external refrigeration unit, which can be easily reflected in economic savings. An almost passive system may also be obtained by designing a PCM-based cooling unit, which is cooled down by an external refrigeration unit and act as cold source by means of a heat transfer fluid and appropriate heat exchangers which let to cool the air inside the refrigerated space. Nevertheless, to design a complete passive system, additional significant studies are necessary. In particular, the refrigeration load needed must be carefully estimated, it must be clearly identified the effects of the cargo inside the refrigerated, how the system reacts to the door openings period, which occurs several times during a normal transportation and distribution activities. Moreover, the proposed systems are usually designed being tuned on the discharging phase, which is, effectively, the most critical phase when dealing with the refrigerated transport. However, in order to push the market to invest in these innovative and more sustainable refrigerated transport solutions, additional analyses regarding the

system as a whole (discharging + charging phases) are vital. In fact, it must be clearly demonstrated that the new proposed idea can ensure the desired transport conditions, but contemporary can be charged in a convenient and cost-effective way. The clear designing of the charging and discharging phases are essential for the development and subsequent spread of a new refrigerated transport application adopting PCMs. Another significant aspect that requires deeply further investigations is the analysis of the relative humidity on the carried foodstuffs. It is well known that humidity can affect the quality and the safety of the cargoes. However, from the retrieved works, only one [89] focused on the study of the relative humidity when a passive PCM based system is employed. It was found that compared to a traditional system, the relative humidity can me maintained at an optimal range (between 80% and 90%) when the passive LTES system is adopted. Additional works are surely needed aiming to extend and verify those results.

It must be also underlined that from the retrieved works, it was not reported if a food precooling is needed before the introduction in the cooling space, and if and how it differs from the precooling level needed for a traditional transport refrigeration system.

Generally, only few works covered the economic advantages deriving from the adoption of a refrigerated system based on PCM. However, significant economic savings reaching values of 80–90% were declared in few works. A detail economic analysis is the fundamental brick to further attract funds and encourage companies in developing such innovative solutions. Nowadays, this aspect acquires more importance due to the growing costs of fuel, which calls the community to find novel alternatives aiming at reducing the operational costs, limiting the impact on the final products prices for the consumers, consequently.

Moreover, since the proposed LTESs must deal with perishable products, such as food, the right selection of the PCM is crucial. It is essential to investigate the effects of a possible PCM leakage in the refrigerated space, in particular, how it would affect the product safety and quality.

Very different external conditions were investigated: such as a real-life profile temperature, constant temperature, single day operating period or a longer one. Additionally, studies covering full-scale applications are extremely needed to demonstrate the practical feasibility and convenience of the novel solutions. Performances close to real conditions, may enhance the confidence of manufacturers to consider the introduction of latent thermal energy storage systems as substitutes of the traditional ones.

The research on PCM based storage portable boxes explored the implementation of multi-temperature PCMs. This smart solution allows to carry multiple products at the same time, reducing cost transportation, thus developing smart distribution chain. The same concept has not been investigated for the refrigerated vehicle, yet. However, it might become an interesting novel concept even in this sector.

Finally, detailed Life Cycle Assessment analyses are strongly required to quantify the environmental benefits and to demonstrate the sustainability of the innovative refrigerated transport systems.

To briefly resume, the main positive and negative aspects regarding the adoption of PCM-based LTES system for the product transportation and distribution sectors along the cold chain are reported as follows.

Compared to a traditional system, a more uniform temperature distribution inside the cold compartment is achievable, which is beneficial for the food quality, especially for foodstuffs carried at positive temperatures, limiting food wastages and losses. Sensible greenhouse gas emissions reduction (up to 90%) can be obtained. The possibility of employing a more efficient stationary cooling unit other than the traditional on-board refrigeration system (low COP) lets to remarkably reduce the operational costs. The LTES can be cooled down by exploiting a renewable energy source, reducing the dependency from fossil fuels. A significant extension of the cooling time of the portable boxes can be reached, which preserves the high-sensible product quality.

On the contrary, the rapid abatement of the heat infiltrations due to door-openings cannot be always easily addressed by a passive PCM-

based system only. Besides, the occurrence of a PCM leakage can be detrimental for the carried foodstuffs. Finally, a LTES system seems more appropriate for a short- or daily- operation route.

Finally, on the basis of the present work, the following gaps can be identified:

- Charging and discharging phases of the LTES systems should be studied and optimized contemporary.
- The effect of the relative humidity on the cold compartment should be considered.
- The effects of the foodstuff precooling should be analyzed.
- Economic analyses to verify the convenience of the LTES system should be prepared.
- A clear and uniform way for the selection of the PCM to be employed should be defined.
- Studies closer to real-life conditions, in terms of external conditions and system sizes should be run.
- Multi-temperature PCMs for refrigerated vehicles can be an option to maximize the advantages of the passive systems.
- Life Cycle Analyses to demonstrate the advantages of the technology for the environment should be considered.

Declaration of Competing Interest

The authors declare that they have no known competing financial interests or personal relationships that could have appeared to influence the work reported in this paper.

Data availability

No data was used for the research described in the article.

References

[1] Food and Agriculture Organization of the United Nations, The State of Food Security and Nutrition in the world : Safeguarding Against Economic Slowdowns and Downturns, International Fund for Agricultural Development, UNICEF, World Food Programme, and World Health Organization, 2022. Accessed: Jun. 03[Online]. Available: https://www.fao.org/3/ca5162en/ca5162en.pdf.

[2] IIR_UN Environment, "Cold Chain Technology Brief: transport Refrigeration," 2018. Accessed: Jun. 03, 2022. [Online]. Available: https://wedocs.unep.org/bitstream/handle/20.500.11822/32571/8142Transpor_Ref_EN.pdf?sequence=1&isAllowed=y.

[3] Jenny. Gustavsson, Food and agriculture organization of the United Nations., and N. ASME/Pacific rim technical conference and exhibition on integration and packaging of MEMS, in: Global food losses and food waste : extent, causes and prevention : study conducted for the International Congress "Save Food!" at Interpack 2011 Düsseldorf, Germany, 2022. Accessed: Jun. 03[Online]. Available: https://www.fao.org/3/mb060e/mb060e00.htm.

[4] UN-environment programme, "Sustainable cold chain and food loss reduction," 2019. Accessed: Jun. 03, 2022. [Online]. Available: https://ozone.unep.org/system/files/documents/MOP31-Sustainable-HL_Briefing_Note.pdf.

[5] Food and Agriculture Organization of the United Nations and Food Wastage Footprint (Project), *Food wastage footprint full-cost accounting : Final report.* Accessed: Jun. 03, 2022. [Online]. Available: https://www.fao.org/3/i3991e/i3991e.pdf.

[6] J.A. Evans, E.C. Hammond, A.J. Gigiel, L. Reinholdt, K. Fikiin, C. Zilio, Assessment of methods to reduce the energy consumption of food cold stores, Appl. Therm. Eng. 62 (2) (2014) 697–705, https://doi.org/10.1016/j.applthermaleng.2013.10.023.

[7] M.A. ben Taher, M. Ahachad, M. Mahdaoui, Y. Zeraouli, T. Kousksou, A survey of computational and experimental studies on refrigerated trucks, J. Energy Storage (2021), https://doi.org/10.1016/j.est.2021.103575. Elsevier Ltd, Mar. 01.

[8] EASE, "Thermal storage position paper," 2017.

[9] H. Jouhara, A. Żabnieńska-Góra, N. Khordehgah, D. Ahmad, T. Lipinski, Latent thermal energy storage technologies and applications: a review, Int. J. Thermofluids 5–6 (Aug. 2020), https://doi.org/10.1016/j.ijft.2020.100039.

[10] M. Mobedi, K. Hooman, W.-.Q. Tao, Solid-Liquid Thermal Energy Storage, CRC Press, Boca Raton, 2022, https://doi.org/10.1201/9781003213260.

[11] Q. Li, X. Ma, X. Zhang, J. Ma, J. Hu, Y. Lan, Microencapsulation of Al-Zn alloy as phase change materials for high-temperature thermal storage application, Mater. Lett. 308 (Feb. 2022), https://doi.org/10.1016/j.matlet.2021.131208.

[12] G. Righetti, L. Doretti, C. Zilio, G.A. Longo, S. Mancin, Experimental investigation of phase change of medium/high temperature paraffin wax embedded in 3D

[13] periodic structure, Int. J. Thermofluids 5–6 (Aug. 2020), https://doi.org/10.1016/j.ijft.2020.100035.

[13] C. Pagkalos, G. Dogkas, M.K. Koukou, J. Konstantaras, K. Lymperis, M.G. Vrachopoulos, Evaluation of water and paraffin PCM as storage media for use in thermal energy storage applications: a numerical approach, Int. J. Thermofluids 1–2 (Feb. 2020), https://doi.org/10.1016/j.ijft.2019.100006.

[14] "https://sunamp.com." https://sunamp.com.

[15] G. Dogkas, et al., Investigating the performance of a thermal energy storage unit with paraffin as phase change material, targeting buildings' cooling needs: an experimental approach, Int. J. Thermofluids 3–4 (May 2020), https://doi.org/10.1016/j.ijft.2020.100027.

[16] I. Dincer and M.A. Rosen, *Exergy analysis of heating, refrigerating and air conditioning.* 2015.

[17] M. Calati, C. Zilio, G. Righetti, G.A. Longo, K. Hooman, S. Mancin, Latent thermal energy storage for refrigerated trucks, Int. J. Refrig. 136 (Apr. 2022) 124–133, https://doi.org/10.1016/j.ijrefrig.2022.01.018.

[18] A. Sharma, V.v. Tyagi, C.R. Chen, D. Buddhi, Review on thermal energy storage with phase change materials and applications, Renew. Sustain. Energy Rev. 13 (2) (Feb. 2009) 318–345, https://doi.org/10.1016/j.rser.2007.10.005.

[19] Y. Yusufoglu, T. Apaydin, S. Yilmaz, H.O. Paksoy, Improving performance of household refrigerators by incorporating phase change materials, Int. J. Refrig. 57 (Jul. 2015) 173–185, https://doi.org/10.1016/j.ijrefrig.2015.04.020.

[20] M.A. Ezan, E. Ozcan Doganay, F.E. Yavuz, I.H. Tavman, A numerical study on the usage of phase change material (PCM) to prolong compressor off period in a beverage cooler, Energy Convers. Manag. 142 (2017) 95–106, https://doi.org/10.1016/j.enconman.2017.03.032.

[21] A. Pirvaram, S.M. Sadrameli, L. Abdolmaleki, Energy management of a household refrigerator using eutectic environmental friendly PCMs in a cascaded condition, Energy 181 (Aug. 2019) 321–330, https://doi.org/10.1016/j.energy.2019.05.129.

[22] B. Gin, M.M. Farid, P.K. Bansal, Effect of door opening and defrost cycle on a freezer with phase change panels, Energy Convers. Manag. 51 (12) (Dec. 2010) 2698–2706, https://doi.org/10.1016/j.enconman.2010.06.005.

[23] Z. Liu, D. Zhao, Q. Wang, Y. Chi, L. Zhang, Étude sur la performance d'un réfrigérateur domestique refroidi par air utilisant des matériaux à changement de phase pour l'entreposage frigorifique, Int. J. Refrig. 79 (Jul. 2017) 130–142, https://doi.org/10.1016/j.ijrefrig.2017.04.009.

[24] E. Oró, L. Miró, M.M. Farid, V. Martin, L.F. Cabeza, Energy management and CO2 mitigation using phase change materials (PCM) for thermal energy storage (TES) in cold storage and transport, Int. J. Refrig. 42 (2014) 26–35, https://doi.org/10.1016/j.ijrefrig.2014.03.002.

[25] "https://www.vikingcold.com/." https://www.vikingcold.com/(accessed Jun. 03, 2022).

[26] P. Schalbart, D. Leducq, G. Alvarez, Ice-cream storage energy efficiency with model predictive control of a refrigeration system coupled to a PCM tank, Int. J. Refrig. 52 (Apr. 2015) 140–150, https://doi.org/10.1016/j.ijrefrig.2014.08.001.

[27] M. Liu, W. Saman, F. Bruno, Development of a novel refrigeration system for refrigerated trucks incorporating phase change material, Appl. Energy 92 (2012) 336–342, https://doi.org/10.1016/j.apenergy.2011.10.015.

[28] B. Michel, P. Glouannec, A. Fuentes, P. Chauvelon, Experimental and numerical study of insulation walls containing a composite layer of PU-PCM and dedicated to refrigerated vehicle, Appl. Therm. Eng. 116 (2017) 382–391, https://doi.org/10.1016/j.applthermaleng.2016.12.117.

[29] T. Lafaye De Micheaux, M. Ducoulombier, J. Moureh, V. Sartre, J. Bonjour, Experimental and numerical investigation of the infiltration heat load during the opening of a refrigerated truck body, Int. J. Refrig. 54 (Jun. 2015) 170–189, https://doi.org/10.1016/j.ijrefrig.2015.02.009.

[30] United Nations. Economic Commission for Europe, Inland transport committee, in: Agreement on the International Carriage of Perishable Foodstuffs and on the Special Equipment to Be Used for Such Carriage (ATP), 2022.

[31] S.A. Tassou, G. De-Lille, Y.T. Ge, Food transport refrigeration - approaches to reduce energy consumption and environmental impacts of road transport, Appl. Therm. Eng. 29 (8–9) (Jun. 2009) 1467–1477, https://doi.org/10.1016/j.applthermaleng.2008.06.027.

[32] G. Li, Comprehensive investigation of transport refrigeration life cycle climate performance, Sustain. Energy Technol. Assessments 21 (Jun. 2017) 33–49, https://doi.org/10.1016/j.seta.2017.04.002.

[33] E. Oró, A. de Gracia, A. Castell, M.M. Farid, L.F. Cabeza, Review on phase change materials (PCMs) for cold thermal energy storage applications, Appl. Energy 99 (2012) 513–533, https://doi.org/10.1016/j.apenergy.2012.03.058.

[34] C. Veerakumar, A. Sreekumar, Phase change material based cold thermal energy storage: materials, techniques and applications - a review, Int. J. Refrig. 67 (Jul. 01, 2016) 271–289, https://doi.org/10.1016/j.ijrefrig.2015.12.005. Elsevier Ltd.

[35] B. Nie, A. Palacios, B. Zou, J. Liu, T. Zhang, Y. Li, Review on phase change materials for cold thermal energy storage applications, Renew. Sustain. Energy Rev. 134 (2020), https://doi.org/10.1016/j.rser.2020.110340. Elsevier Ltd, Dec. 01.

[36] Y. Zhao, X. Zhang, X. Xu, S. Zhang, Research progress of phase change cold storage materials used in cold chain transportation and their different cold storage packaging structures, J. Mol. Liq. 319 (2020), https://doi.org/10.1016/j.molliq.2020.114360. Elsevier B.V., Dec. 01.

[37] H. Selvnes, Y. Allouche, R.I. Manescu, A. Hafner, Review on cold thermal energy storage applied to refrigeration systems using phase change materials, Therm. Sci. Eng. Progress 22 (2021), https://doi.org/10.1016/j.tsep.2020.100807. Elsevier Ltd, May 01.

[38] Z. Yin, J. Zheng, H. Kim, Y. Seo, P. Linga, Hydrates for cold energy storage and transport: a review, Adv. Appl. Energy 2 (May 2021), 100022, https://doi.org/10.1016/j.adapen.2021.100022.

[39] G. Hameed, et al., Low temperature phase change materials for thermal energy storage: current status and computational perspectives, Sustain. Energy Technol. Assessments 50 (Mar. 2022), https://doi.org/10.1016/j.seta.2021.101808.

[40] T. Leungtongkum, D. Flick, H.M. Hoang, D. Steven, A. Delahaye, O. Laguerre, Insulated box and refrigerated equipment with PCM for food preservation: state of the art, J. Food Eng. 317 (2022), https://doi.org/10.1016/j.jfoodeng.2021.110874. Elsevier Ltd, Mar. 01.

[41] A.P. Simard and M. Lacroix, "Study of the thermal behavior of a latent heat cold storage unit operating under frosting conditions." [Online]. Available: www.elsevier.com/locate/enconman.

[42] X. Li, S. Yang, D. Zhou, Study of new cool storage materials for refrigerated vehicle in cold chain, in: 2010 International Conference on Logistics Systems and Intelligent Management, ICLSIM 2010 2, 2010, pp. 637–640, https://doi.org/10.1109/ICLSIM.2010.5461341.

[43] L. Melone, L. Altomare, A. Cigada, L. de Nardo, Phase change material cellulosic composites for the cold storage of perishable products: from material preparation to computational evaluation, Appl. Energy 89 (1) (2012) 339–346, https://doi.org/10.1016/j.apenergy.2011.07.039.

[44] W. Lu, S.A. Tassou, Characterization and experimental investigation of phase change materials for chilled food refrigerated cabinet applications, Appl. Energy 112 (2013) 1376–1382, https://doi.org/10.1016/j.apenergy.2013.01.071.

[45] A. Sari, A. Karaipekli, R. Eroğlu, A. Biçer, Erythritol tetra myristate and erythritol tetra laurate as novel phase change materials for low temperature thermal energy storage, Energy Sources Part A Recov. Utiliz. Environ. Effects 35 (14) (Jul. 2013) 1285–1295, https://doi.org/10.1080/15567036.2010.516323.

[46] R. Pérez-Masiá, A. López-Rubio, M.J. Fabra, J.M. Lagaron, Use of electrohydrodynamic processing to develop nanostructured materials for the preservation of the cold chain, Innovative Food Sci. Emerg. Technol. 26 (Dec. 2014) 415–423, https://doi.org/10.1016/j.ifset.2014.10.010.

[47] P. Han, L. Lu, X. Qiu, Y. Tang, J. Wang, Preparation and characterization of macrocapsules containing microencapsulated PCMs (phase change materials) for thermal energy storage, Energy 91 (Nov. 2015) 531–539, https://doi.org/10.1016/j.energy.2015.08.001.

[48] J. Chen, P. Zhang, Preparation and characterization of nano-sized phase change emulsions as thermal energy storage and transport media, Appl. Energy 190 (2017) 868–879, https://doi.org/10.1016/j.apenergy.2017.01.012.

[49] A. Coca-Ortegón, V. Torres-Toledo, J. Müller, A. Coronas, PAPER ID 10796 assessment of a solar powered refrigerator equipped with thermal storage for a dairy application, in: ISES Solar World Congress 2017 - IEA SHC International Conference on Solar Heating and Cooling for Buildings and Industry 2017, Proceedings, 2017, pp. 1655–1666, https://doi.org/10.18086/swc.2017.28.02.

[50] D.W. Lee, Experimental study on performance characteristics of cold storage heat exchanger for ISG vehicle, Int. J. Automotive Technol. 18 (1) (2017) 41–48, https://doi.org/10.1007/s12239−017−0004−x.

[51] F. Ma, P. Zhang, X.J. Shi, Investigation of thermo-fluidic performance of phase change material slurry and energy transport characteristics, Appl. Energy 227 (Oct. 2018) 643–654, https://doi.org/10.1016/j.apenergy.2017.08.146.

[52] L.R. Soenksen, D.A. Martínez-Corona, S.I. de Gante, P.S. Phabmixay, M.J. M. Maggi, Low-cost thermal shield for rapid diagnostic tests using phase change materials, J. Med. Devices, Trans. ASME 12 (1) (Mar. 2018), https://doi.org/10.1115/1.4038898.

[53] L. Cong, X. She, G. Leng, G. Qiao, C. Li, Y. Ding, Formulation and characterisation of ternary salt based solutions as phase change materials for cold chain applications, Energy Procedia 158 (2019) 5103–5108, https://doi.org/10.1016/j.egypro.2019.01.690.

[54] Y. Li, X. Zhang, J.M. Munyalo, Z. Tian, J. Ji, Preparation and thermophysical properties of low temperature composite phase change material octanoic-lauric acid/expanded graphite, J. Mol. Liq. 277 (Mar. 2019) 577–583, https://doi.org/10.1016/j.molliq.2018.12.111.

[55] Y. Song, N. Zhang, Y. Jing, X. Cao, Y. Yuan, F. Haghighat, Experimental and numerical investigation on dodecane/expanded graphite shape-stabilized phase change material for cold energy storage, Energy 189 (Dec. 2019), https://doi.org/10.1016/j.energy.2019.116175.

[56] Y. Wang, et al., Thermal conductivity modification of n-octanoic acid-myristic acid composite phase change material, J. Mol. Liq. 288 (Aug. 2019), https://doi.org/10.1016/j.molliq.2019.111092.

[57] V.J. Reddy, J.S. Yadav, S. Chattopadhyay, Phase change material loaded form-stable composites for low temperature thermal buffering application, Mater. Chem. Phys. 247 (Jun. 2020), https://doi.org/10.1016/j.matchemphys.2020.122859.

[58] T. Wu, et al., Preparation of a low-temperature nanofluid phase change material: mgCl2−H2O eutectic salt solution system with multi-walled carbon nanotubes (MWCNTs),", Int. J. Refrig. 113 (May 2020) 136–144, https://doi.org/10.1016/j.ijrefrig.2020.02.008.

[59] N. Xie, Z. Li, X. Gao, Y. Fang, Z. Zhang, Preparation and performance of modified expanded graphite/eutectic salt composite phase change cold storage material, Int. J. Refrig. 110 (Feb. 2020) 178–186, https://doi.org/10.1016/j.ijrefrig.2019.10.008.

[60] S. Zhang, X. Zhang, X. Xu, and Y. Zhao, "Experimental study on the storage and release characteristics of phase change materials with different nanomaterials as addictives", doi: 10.1007/s00231-020-02882-1/Published.

[61] S. Zhang, X. Zhang, X. Xu, Y. Zhao, Preparation and properties of decyl–myristyl alcohol/expanded graphite low temperature composite phase change material, Phase Transitions 93 (5) (May 2020) 491–503, https://doi.org/10.1080/01411594.2020.1758319.

[62] J. Zhao, et al., Recyclable low-temperature phase change microcapsules for cold storage, J. Colloid Interface Sci. 564 (Mar. 2020) 286–295, https://doi.org/10.1016/j.jcis.2019.12.037.

[63] M. Berdja, J. Hu, A. Hamid, O. Sari, Investigation on the anti-supercooling effect of sodium polyacrylate as an additive in phase change materials for the applications of latent heat thermal energy storage, J. Energy Storage 36 (Apr. 2021), https://doi.org/10.1016/j.est.2021.102397.

[64] W. Beyne, K. Couvreur, S. Lecompte, M. de Paepe, A technical, financial and CO2 emission analysis of the implementation of metal foam in a thermal battery for cold chain transport, J. Energy Storage 35 (Mar. 2021), https://doi.org/10.1016/j.est.2021.102324.

[65] J. Ji, Y. Wang, X. Lin, B. Liu, X. Zhang, Fabrication of highly thermal conductive and shape-stabilized phase change materials, J. Energy Storage 44 (Dec. 2021), https://doi.org/10.1016/j.est.2021.103256.

[66] N. Lin, C. Li, D. Zhang, Y. Li, J. Chen, Enhanced cold storage performance of Na2SO4·10H2O/expanded graphite composite phase change materials, Sustain. Energy Technol. Assessments 48 (Dec. 2021), https://doi.org/10.1016/j.seta.2021.101596.

[67] X. Qiu, L. Lu, Microencapsulated paraffin as a phase change material with polyurea/polyurethane/poly(lauryl methacrylate) hybrid shells for thermal energy storage applications, J. Renew. Sustain. Energy 13 (1) (Jan. 2021), https://doi.org/10.1063/5.0025731.

[68] C.E. Tas, H. Unal, Thermally buffering polyethylene/halloysite/phase change material nanocomposite packaging films for cold storage of foods, J. Food Eng. 292 (Mar. 2021), https://doi.org/10.1016/j.jfoodeng.2020.110351.

[69] D. Zhan, et al., Phase change material for the cold storage of perishable products: from material preparation to material evaluation, J. Mol. Liq. 342 (Nov. 2021), https://doi.org/10.1016/j.molliq.2021.117455.

[70] L. Zhao, et al., Preparation and thermal properties of low-temperature composite phase-change materials based on a binary eutectic mixture with expanded graphite: effect of particle size and mass fraction, J. Energy Storage 40 (Aug. 2021), https://doi.org/10.1016/j.est.2021.102778.

[71] Y. Zhao, X. Zhang, X. Xu, Application and research progress of cold storage technology in cold chain transportation and distribution, J. Therm. Anal. Calorim. 139 (2) (2020) 1419–1434, https://doi.org/10.1007/s10973-019-08400-8. Springer NetherlandsJan. 01.

[72] N. Lin, C. Li, D. Zhang, Y. Li, J. Chen, Emerging phase change cold storage materials derived from sodium sulfate decahydrate, Energy 245 (Apr. 2022), 123294, https://doi.org/10.1016/j.energy.2022.123294.

[73] L. Liu, X. Zhang, X. Lin, Experimental investigations on the thermal performance and phase change hysteresis of low-temperature paraffin/MWCNTs/SDBS nanocomposite via dynamic DSC method, Renew. Energy 187 (Mar. 2022) 572–585, https://doi.org/10.1016/j.renene.2022.01.098.

[74] H.H. MERT, B. KEKEVİ, E.H. MERT, M.S.. M.ERT, Development of composite phase change materials based on n-tetradecane and β-myrcene based foams for cold thermal energy storage applications, Thermochim. Acta 707 (Jan. 2022), https://doi.org/10.1016/j.tca.2021.179116.

[75] Y. Pu, J. Fang, Y. Du, Preparation and characterization of reusable water/ethylcellulose phase change cold storage microcapsules with high latent heat, Colloids Surf. A Physicochem. Eng. Asp. 633 (Jan. 2022), https://doi.org/10.1016/j.colsurfa.2021.127833.

[76] M. Ahmed, O. Meade, M.A. Medina, Reducing heat transfer across the insulated walls of refrigerated truck trailers by the application of phase change materials, Energy Convers. Manag. 51 (3) (Mar. 2010) 383–392, https://doi.org/10.1016/j.enconman.2009.09.003.

[77] H. Tan, Y. Li, H. Tuo, M. Zhou, B. Tian, Experimental study on liquid/solid phase change for cold energy storage of liquefied natural gas (LNG) refrigerated vehicle, Energy 35 (5) (2010) 1927–1935, https://doi.org/10.1016/j.energy.2010.01.006.

[78] E. Oró, L. Miró, M.M. Farid, L.F. Cabeza, Thermal analysis of a low temperature storage unit using phase change materials without refrigeration system, Int. J. Refrig. 35 (6) (Sep. 2012) 1709–1714, https://doi.org/10.1016/j.ijrefrig.2012.05.004.

[79] P. Glouannec, B. Michel, G. Delamarre, Y. Grohens, Experimental and numerical study of heat transfer across insulation wall of a refrigerated integral panel van, Appl. Therm. Eng. 73 (1) (Dec. 2014) 196–204, https://doi.org/10.1016/j.applthermaleng.2014.07.044.

[80] M. Liu, W. Saman, F. Bruno, Computer simulation with TRNSYS for a mobile refrigeration system incorporating a phase change thermal storage unit, Appl. Energy 132 (Nov. 2014) 226–235, https://doi.org/10.1016/j.apenergy.2014.06.066.

[81] A. Tinti, A. Tarzia, A. Passaro, R. Angiuli, Thermographic analysis of polyurethane foams integrated with phase change materials designed for dynamic thermal insulation in refrigerated transport, Appl. Therm. Eng. 70 (1) (Sep. 2014) 201–210, https://doi.org/10.1016/j.applthermaleng.2014.05.003.

[82] R. Sepe, E. Armentani, A. Pozzi, Development and stress behaviour of an innovative refrigerated container with PCM for fresh and frozen goods, Multidiscipline Model. Mater. Structures 11 (2) (Aug. 2015) 202–215, https://doi.org/10.1108/MMMS-05-2014-0030.

[83] B. Copertaro, P. Principi, R. Fioretti, Thermal performance analysis of PCM in refrigerated container envelopes in the Italian context - Numerical modeling and validation, Appl. Therm. Eng. 102 (Jun. 2016) 873–881, https://doi.org/10.1016/j.applthermaleng.2016.04.050.

[84] R. Fioretti, P. Principi, B. Copertaro, A refrigerated container envelope with a PCM (Phase Change Material) layer: experimental and theoretical investigation in a representative town in Central Italy, Energy Convers. Manag. 122 (Aug. 2016) 131–141, https://doi.org/10.1016/j.enconman.2016.05.071.

[85] P. Principi, R. Fioretti, B. Copertaro, Energy saving opportunities in the refrigerated transport sector through phase change materials (PCMs) application, in: Journal of Physics: Conference Series 923, Nov. 2017, https://doi.org/10.1088/1742-6596/923/1/012043.

[86] B. Nie, et al., Experimental study of charging a compact PCM energy storage device for transport application with dynamic exergy analysis, Energy Convers. Manag. 196 (Sep. 2019) 536–544, https://doi.org/10.1016/j.enconman.2019.06.032.

[87] A. Mousazade, R. Rafee, M.S. Valipour, Thermal performance of cold panels with phase change materials in a refrigerated truck, Int. J. Refrig. 120 (Dec. 2020) 119–126, https://doi.org/10.1016/j.ijrefrig.2020.09.003.

[88] M.A. ben Taher, T. Kousksou, Y. Zeraouli, M. Ahachad, M. Mahdaoui, Thermal performance investigation of door opening and closing processes in a refrigerated truck equipped with different phase change materials, J. Energy Storage 42 (Oct. 2021), https://doi.org/10.1016/j.est.2021.103097.

[89] S. Tong, et al., A phase change material (PCM) based passively cooled container for integrated road-rail cold chain transportation – An experimental study, Appl. Therm. Eng. 195 (Aug. 2021), https://doi.org/10.1016/j.applthermaleng.2021.117204.

[90] J.H. Ahn, H. Kim, Y. Jeon, K.H. Kwon, Performance characteristics of mobile cooling system utilizing ice thermal energy storage with direct contact discharging for a refrigerated truck, Appl. Energy 308 (Feb. 2022), https://doi.org/10.1016/j.apenergy.2021.118373.

[91] K. Zdun, T. Uhl, Improvement of properties of an insulated wall for refrigerated trailer-numerical and experimental study, Energies (Basel) 15 (1) (Jan. 2022), https://doi.org/10.3390/en15010051.

[92] Y. Kozak, M. Farid, G. Ziskind, Experimental and comprehensive theoretical study of cold storage packages containing PCM, Appl. Therm. Eng. (2017) 899–912.

[93] L. Huang, U. Piontek, Improving performance of cold-chain insulated container with phase change material: an experimental investigation, Appl. Sci. (Switzerland) 7 (12) (Dec. 2017), https://doi.org/10.3390/app7121288.

[94] J. Du, B. Nie, Y. Zhang, Z. Du, li Wang, Y. Ding, Cooling performance of a thermal energy storage-based portable box for cold chain applications, J. Energy Storage 28 (Apr. 2020), https://doi.org/10.1016/j.est.2020.101238.

[95] B. Nie, et al., Thermal performance enhancement of a phase change material (PCM) based portable box for cold chain applications, J. Energy Storage 40 (Aug. 2021), https://doi.org/10.1016/j.est.2021.102707.

[96] Y. Zhao, X. Zhang, X. Xu, S. Zhang, Development of composite phase change cold storage material and its application in vaccine cold storage equipment, J. Energy Storage 30 (Aug. 2020), https://doi.org/10.1016/j.est.2020.101455.

[97] A.K. Ray, S. Singh, D. Rakshit, Udayraj, Comparative study of cooling performance for portable cold storage box using phase change medium, Therm. Sci. En. Progress 27 (Jan. 2022), 101146, https://doi.org/10.1016/j.tsep.2021.101146.

[98] X. Xu, X. Zhang, S. Liu, Experimental study on cold storage box with nanocomposite phase change material and vacuum insulation panel, Int. J. Energy Res. 42 (14) (Nov. 2018) 4429–4438, https://doi.org/10.1002/er.4187.

[99] X. Xiaofeng, Z. Xuelai, Simulation and experimental investigation of a multi-temperature insulation box with phase change materials for cold storage, J. Food Eng. 292 (Mar. 2021), https://doi.org/10.1016/j.jfoodeng.2020.110286.

[100] J. Guo, J. Liu, J. Ren, Z. Zeng, E. Lü, Experimental study on thermal storage characteristics of cold storage distribution box, J. Energy Storage 55 (Nov. 2022), https://doi.org/10.1016/j.est.2022.105475.

[101] E. Oró, A. de Gracia, L.F. Cabeza, Active phase change material package for thermal protection of ice cream containers, Int. J. Refrig. 36 (1) (Jan. 2013) 102–109, https://doi.org/10.1016/j.ijrefrig.2012.09.011.

[102] D. Leducq, F.T. Ndoye, G. Alvarez, Phase change material for the thermal protection of ice cream during storage and transportation, Int. J. Refrig. 52 (Apr. 2015) 133–139, https://doi.org/10.1016/j.ijrefrig.2014.08.012.

[103] G. Liu, et al., Improving system performance of the refrigeration unit using phase change material (PCM) for transport refrigerated vehicles: an experimental investigation in South China, J. Energy Storage 51 (Jul. 2022), https://doi.org/10.1016/j.est.2022.104435.

[104] S. Burgess, X. Wang, A. Rahbari, M. Hangi, Optimisation of a portable phase-change material (PCM) storage system for emerging cold-chain delivery applications, J. Energy Storage 52 (Aug. 2022), https://doi.org/10.1016/j.est.2022.104855.

[105] K. Liu, et al., Highly-efficient cold energy storage enabled by brine phase change material gels towards smart cold chain logistics, J. Energy Storage 52 (Aug. 2022), https://doi.org/10.1016/j.est.2022.104828.

[106] Y. Cao, et al., Designing a system for battery thermal management: cooling LIBs by nano-encapsulated phase change material, Case Stud. Therm. Eng. 33 (May 2022), 101943, https://doi.org/10.1016/j.csite.2022.101943.

[107] X. Xiao, P. Zhang, M. Li, Preparation and thermal characterization of paraffin/metal foam composite phase change material, Appl. Energy 112 (2013) 1357–1366, https://doi.org/10.1016/j.apenergy.2013.04.050.

[108] S. Yu, X. Wang, D. Wu, Microencapsulation of n-octadecane phase change material with calcium carbonate shell for enhancement of thermal conductivity and serving durability: synthesis, microstructure, and performance evaluation, Appl. Energy 114 (2014) 632–643, https://doi.org/10.1016/j.apenergy.2013.10.029.

[109] G. Liu, et al., Design and assessments on a hybrid pin fin-metal foam structure towards enhancing melting heat transfer: an experimental study, Int. J. Therm. Sci. 182 (Dec. 2022), https://doi.org/10.1016/j.ijthermalsci.2022.107809.

[110] F. Bruno, M. Belusko, M. Liu, N.H.S. Tay, Using solid-liquid phase change materials (PCMs) in thermal energy storage systems. Advances in Thermal Energy Storage Systems: Methods and Applications, Elsevier Inc., 2015, pp. 201–246, https://doi.org/10.1533/9781782420965.2.201.

[111] X. Zhang, J. Niu, J.Y. Wu, Development and characterization of novel and stable silicon nanoparticles-embedded PCM-in-water emulsions for thermal energy storage, Appl. Energy 238 (Mar. 2019) 1407–1416, https://doi.org/10.1016/j.apenergy.2019.01.159.

[112] F. Wang, C. Zhang, J. Liu, X. Fang, Z. Zhang, Highly stable graphite nanoparticle-dispersed phase change emulsions with little supercooling and high thermal conductivity for cold energy storage, Appl. Energy 188 (2017) 97–106, https://doi.org/10.1016/j.apenergy.2016.11.122.

[113] H. Mehling and C. Luisa F, Heat and Cold Storage with PCM. 2008.

[114] M.M. Farid, A.M. Khudhair, S.A.K. Razack, S. Al-Hallaj, A review on phase change energy storage: materials and applications, Energy Conversion and Manag. 45 (9–10) (Jun. 2004) 1597–1615, https://doi.org/10.1016/j.enconman.2003.09.015.

[115] L.F. Cabeza, G. Svensson, S. Hiebler, H. Mehling, Thermal performance of sodium acetate trihydrate thickened with different materials as phase change energy storage material, Appl. Therm. Eng. 23 (13) (Aug. 2003) 1697–1704, https://doi.org/10.1016/S1359-4311(03)00107-8.

[116] Z. Wang, et al., Preparation and properties of caprylic-nonanoic acid mixture/expanded graphite composite as phase change material for thermal energy storage, Int. J. Energy Res. 41 (15) (Dec. 2017) 2555–2564, https://doi.org/10.1002/er.3830.

[117] E. Oró, L. Miró, C. Barreneche, I. Martorell, M.M. Farid, L.F. Cabeza, Corrosion of metal and polymer containers for use in PCM cold storage, Appl. Energy 109 (2013) 449–453, https://doi.org/10.1016/j.apenergy.2012.10.049.

[118] G. Ferrer, A. Solé, C. Barreneche, I. Martorell, L.F. Cabeza, Corrosion of metal containers for use in PCM energy storage, Renew. Energy 76 (Apr. 2015) 465–469, https://doi.org/10.1016/j.renene.2014.11.036.

[119] A.J. Farrell, B. Norton, D.M. Kennedy, Corrosive effects of salt hydrate phase change materials used with aluminium and copper, J. Mater. Process. Technol. 175 (1–3) (Jun. 2006) 198–205, https://doi.org/10.1016/j.jmatprotec.2005.04.058.

[120] S.S. Chandel, T. Agarwal, Review of current state of research on energy storage, toxicity, health hazards and commercialization of phase changing materials, Renew. Sustain. Energy Rev. 67 (Jan. 01, 2017) 581–596, https://doi.org/10.1016/j.rser.2016.09.070. Elsevier Ltd.

[121] "https://www.crodaenergytechnologies.com/en-gb/product-finder/product/1382-CrodaTherm_1_9.5." https://www.crodaenergytechnologies.com/en-gb/product-finder/product/1382-CrodaTherm_1_9.5 (accessed Jun. 03, 2022).

[122] "https://www.iso.org/standard/37456.html." https://www.iso.org/standard/37456.html (accessed Jun. 03, 2022).

[123] B.R. David, S. Spencer, J. Miller, S. Almahmoud, H. Jouhara, Comparative environmental life cycle assessment of conventional energy storage system and innovative thermal energy storage system, Int. J. Thermofluids 12 (Nov. 2021), https://doi.org/10.1016/j.ijft.2021.100116.

[124] P. Duggal, R.K. Tomar, N.D. Kaushika, A Review on life cycle assessment of phase change materials in buildings, in: Proceedings of 2021 2nd International Conference on Intelligent Engineering and Management, ICIEM 2021, Apr. 2021, pp. 18–22, https://doi.org/10.1109/ICIEM51511.2021.9445375.

[125] E. Kyriaki, C. Konstantinidou, E. Giama, A.M. Papadopoulos, Life cycle analysis (LCA) and life cycle cost analysis (LCCA) of phase change materials (PCM) for thermal applications: a review, Int. J. Energy Res. 42 (9) (Jul. 2018) 3068–3077, https://doi.org/10.1002/er.3945.

[126] B. Behdani, Y. Fan, J.M. Bloemhof, Cool chain and temperature-controlled transport: an overview of concepts, challenges, and technologies. Sustainable Food Supply Chains: Planning, Design, and Control through Interdisciplinary Methodologies, Elsevier, 2019, pp. 167–183, https://doi.org/10.1016/B978-0-12-813411-5.00012-0.

[127] American Society of Heating Refrigerating and Air-Conditioning Engineers, in: 2018 ASHRAE handbook : refrigeration, 2022.

[128] S. Estrada-Flores, A. Eddy, Thermal performance indicators for refrigerated road vehicles, Int. J. Refrig. 29 (6) (Sep. 2006) 889–898, https://doi.org/10.1016/j.ijrefrig.2006.01.012.

[129] D.Y. Lee, V.M. Thomas, M.A. Brown, Electric urban delivery trucks: energy use, greenhouse gas emissions, and cost-effectiveness, Environ. Sci. Technol. 47 (14) (Jul. 2013) 8022–8030, https://doi.org/10.1021/es400179w.

[130] M. Calati, L. Doretti, C. Zilio, S. Mancin, 3D numerical simulation of a novel ventilated roof: thermal performance analysis and fluid flow behavior, Sci. Technol. Built. Environ. 27 (6) (2021) 819–831, https://doi.org/10.1080/23744731.2021.1917931.

[131] UNI 10349, Heating and cooling of buildings, Climatic data, Italian Standard,1994.

[132] R. Chandran, M. Hasanuzzaman, M. Arıcı, L. Kumar, Energy, economic and environmental impact analysis of phase change materials for cold chain

transportation in Malaysia, J. Energy Storage 55 (Nov. 2022), https://doi.org/10.1016/j.est.2022.105481.

[133] T.B. Radebe, Z. Huan, J. Baloyi, Simulation of eutectic plates in medium refrigerated transport, J. Eng. Design and Technol. 19 (1) (Mar. 2021) 62–80, https://doi.org/10.1108/JEDT-02-2020-0065.

[134] J. Jeong, A.E. Benchikh Le Hocine, S. Croquer, S. Poncet, B. Michel, J. Bonjour, Numerical analysis of the thermoaeraulic behavior of air during the opening of the door of a refrigerated truck trailer equipped with cold plates, Appl. Therm. Eng. 206 (Apr. 2022), 118057, https://doi.org/10.1016/j.applthermaleng.2022.118057.